Downloaded from orbit.dtu.dk on: Mar 24, 2025

DTU Library

Heat and water transport in soils and across the soil-atmosphere interface: 1. Theory and different model concepts

Vanderborght, Jan; Fetzer, Thomas; Mosthaf, Klaus; Smits, Kathleen M.; Helmig, Rainer

Published in:
Water Resources Research

Link to article, DOI:
10.1002/2016WR019982

Publication date:
2017

Document Version
Peer reviewed version

Link back to DTU Orbit

Citation (APA):
Vanderborght, J., Fetzer, T., Mosthaf, K., Smits, K. M., & Helmig, R. (2017). Heat and water transport in soils and across the soil-atmosphere interface: 1. Theory and different model concepts. *Water Resources Research*, *53*(2), 1057-1079. https://doi.org/10.1002/2016WR019982

General rights
Copyright and moral rights for the publications made accessible in the public portal are retained by the authors and/or other copyright owners and it is a condition of accessing publications that users recognise and abide by the legal requirements associated with these rights.

- Users may download and print one copy of any publication from the public portal for the purpose of private study or research.
- You may not further distribute the material or use it for any profit-making activity or commercial gain
- You may freely distribute the URL identifying the publication in the public portal

If you believe that this document breaches copyright please contact us providing details, and we will remove access to the work immediately and investigate your claim.

Heat and water transport in soils and across the soil-atmosphere interface – Part 1: Theory and different model concepts.

Jan Vanderborght[1,2*], Thomas Fetzer[3], Klaus Mosthaf[4], Kathleen Smits[5], Rainer Helmig[3].

[1] Agrosphere Institute, IBG-3, Forschungszentrum Jülich GmbH, D-52425 Jülich, Germany. j.vanderborght@fz-juelich.de

[2] Centre for High-Performance Scientific Computing in Terrestrial Systems, HPSC TerrSys, Geoverbund ABCJ, Forschungszentrum Jülich GmbH, D-52425 Jülich.

[3] Institute for Modelling Hydraulic and Environmental Systems, University of Stuttgart, Pfaffenwaldring 61, 70569 Stuttgart, Germany. Thomas.Fetzer@iws.uni-stuttgart.de, Rainer.Helmig@iws.uni-stuttgart.de

[4] DTU ENVIRONMENT, Department of Environmental Engineering, Technical University of Denmark, Bygningstorvet, Building 115, 2800 Kgs. Lyngby, Denmark. klmos@env.dtu.dk

[5] Center for Experimental Study of Subsurface Environmental processes, Department of Civil & Environmental Engineering, Colorado Schools of Mines, 1500 Illinois Street, Golden, CO 80401, USA. ksmits@mines.edu

* corresponding author

Abstract

- We review theory and model concepts for evaporation from porous media.
- We discuss the underlying assumptions and simplifications of different approaches.
- Approaches differ in the description of lateral transport, transport in the air phase of the porous medium, and coupling at the porous medium free flow interface.

Abstract

Evaporation is an important component of the soil water balance. It is comprised of water flow and transport processes in a porous medium that are coupled with heat fluxes and free air flow. This work provides a comprehensive review of model concepts used in different research fields to describe evaporation. Concepts range from non-isothermal two-phase flow, two-component transport in the porous medium that is coupled with one-phase flow, two-component transport in the free air flow to isothermal liquid water flow in the porous medium with upper boundary conditions defined by a potential evaporation flux when available energy and transfer to the free airflow are limiting or by a critical threshold water pressure when soil water availability is limiting. The latter approach corresponds with the classical Richards equation with mixed boundary conditions. We compare the different approaches on a theoretical level by identifying the underlying simplifications that are made for the different compartments of the system: porous medium, free flow and their interface, and by discussing how processes not explicitly considered are parameterized. Simplifications can be grouped into three sets depending on whether lateral variations in vertical fluxes are considered, whether flow and transport in the air phase in the porous medium are considered, and depending on how the interaction at the interface between the free flow and the porous medium is represented. The consequences of the simplifications are illustrated by numerical simulations in an accompanying paper.

Introduction

The primary exchanges of heat and water that motivate global and local meteorological conditions occur at the Earth's surface. Many weather and climate phenomena (e.g., monsoons and droughts) are primarily influenced by processes associated with land-atmosphere interactions in which soil moisture and its control on evapotranspiration plays an important role [*Seneviratne et al.*, 2006]. More than half of the Earth's surface is arid or semiarid having little to no vegetative cover [*Katata et al.*, 2007; *Verstraete and Schwartz*, 1991; *Warren*, 1996]. In addition, over 40% of the Earth's terrestrial surface is devoted to agricultural purposes, much of which, due to tillage practices, is bare over a substantial period of the year. Properly describing the water cycle on the basis of heat and water exchanges between the atmosphere and the soil surface is paramount to improving the understanding of water balance conditions in these regions. Despite the importance of these predictions, standard models vary in their ability to predict water fluxes, flow pathways and water distribution. For instance, the fraction of globally averaged evaporation from the soil surface to the total evapotranspiration from the land surface (i.e. including transpiration by the vegetation) varies for different land surface models between 36% and 75% [*Wang and Dickinson*, 2012] with a mean of 58%.

Understanding and controlling evaporation rates from soil is also important at much smaller scales for the water management of cropped soils. For instance, in rain fed agriculture in semiarid regions, where fields are cropped only once every two years and water is harvested during the non-cropped year, evaporation losses during the non-cropped year determine the process or practice efficiency. Evaporation may be reduced in several ways. First, by tillage, capillaries or fine pores that connect the evaporating soil surface with the water stored deeper in the soil are disrupted, potentially decreasing evaporation fluxes. Nevertheless, tillage may bring deeper wet soil to the soil surface therefore increasing the evaporation losses. In addition, vapor diffusion may be facilitated through the large interaggregate pores in tilled soils. The rougher surface of a tilled soil may also affect

reflectivity (albedo) and net radiation [*Potter et al.*, 1987] and the vapor transfer between the soil surface and the atmosphere. Tillage-affected soil structure alter the evaporation behavior depending on the weather conditions and may either lead to larger or smaller evaporation losses [*Moret et al.*, 2007; *Sillon et al.*, 2003; *Unger and Cassel*, 1991]. Another way to reduce evaporation from soil is through a drying concept known as "self-mulching", referring to the development of a dry layer within the soil, which transfers moisture only in the vapor phase [*Li et al.*, 2016; *Novak*, 2010]. This naturally formed layer represents an effective way to maintain soil moisture in the subsurface and it can be improved artificially by applying non-natural mulching materials, such as gravel or plastic, to the soil surface in arid/semi-arid regions or in various horticultural systems [*Chung and Horton*, 1987; *Modaihsh et al.*, 1985; *Tarara and Ham*, 1999; *Yamanaka et al.*, 2004]. The physical mechanism is a hygroscopic equilibrium between the soil vapor pressure and the atmospheric humidity, minimizing the evaporation from the mulch [*Fuchs and Hadas*, 2011]. Several experimental studies have been conducted to investigate the effects of mulch properties on soil surface evaporation processes [*Diaz et al.*, 2005; *Xie et al.*, 2006; *Yuan et al.*, 2009]. A negative correlation between evaporation reduction ability and grain size as well as a positive correlation with mulch thickness has been recognized through sensitivity analyses of experimental results. *Or et al.* [2013] reviewed the physical processes that control evaporation processes from porous media and focused on the role of capillary and viscous forces and of diffusive transfers in the porous medium and across the interface between the porous medium and the free flow. This approach allowed them to relate evaporation process to microscopic properties of the porous medium. In simulation models that operate at the continuum scale, these small scale processes and properties must be included in macroscopic properties and constitutive relations between properties, states and fluxes.

Practical and theoretical limitations of modeling efforts at the continuum scale are often magnified at the land-atmosphere interface, where water and energy fluxes are highly dynamic and dramatically influenced by changes in temperature and moisture gradients and direction of flows

[*Lehmann et al.*, 2012]. The flow and transport behavior at the soil surface is affected by the conditions in the atmosphere (e.g., humidity, temperature, wind velocity, solar radiation) and by the soil thermal and hydraulic properties and states (e.g., thermal and hydraulic conductivity, porosity, capillary pressure, temperature, vapor pressure), all of which are strongly coupled [*Sakai et al.*, 2011]. For most subsurface models, the soil surface serves as the upper boundary to the porous medium domain and is characterized using prescribed flux terms that serve as sources and sinks. Similarly, in most atmospheric models, the vadose zone serves as a lower boundary with prescribed fluxes. Such an approach is a simplification of the interaction processes at the common interface of the two flow compartments. Although widely used due to its simplicity and ease of use, such an approach has been shown by both atmospheric and hydrogeological scientists to misrepresent flux conditions, resulting in model prediction errors [*Seager et al.*, 2007].

In practice, the Richards equation is the most frequently used conceptual model to describe water movement within the vadose zone, and to simulate water and energy exchanges between the land surface and the atmosphere at the global scale. However, it is mostly used in a form that considers only isothermal liquid water flow but neglects vapor diffusion and air flow in the porous medium and the effects of temperature gradients on flow and transport processes. Although the application of Richards equation has been successful to describe soil water fluxes at various scales (e.g. [*Mortensen et al.*, 2006; *Nieber and Walter*, 1981; *Schoups et al.*, 2005; *Vereecken et al.*, 1991]), there may arise conditions in which the non-considered processes become relevant. The predictive capacities of the Richards equation to evaluate, for instance, surface manipulations that influence air flow, vapor transport and thermal regimes in the porous medium could therefore be questioned. Also for global scale simulations, the consideration of additional processes such as vapor transport in the soil and transport driven by thermal gradients are receiving more attention to reduce the bias in bare soil evaporation predictions that are observed in these models [*Tang and Riley*, 2013b].

Most Richards equation based models assume that soil water flux is one-dimensional (i.e. water flow only occurs vertically), thus neglecting any lateral variations in fluxes within the soil profiles

and also at the soil-atmosphere interface. Three-dimensional solutions of the Richards equation have been used to investigate the effect of soil heterogeneity and hence dimensionality on flow and transport processes. However, these simulation studies focused mostly on conditions when flow was directed downward (infiltration). For certain problems of practical relevance, e.g. evaporation from surfaces that are partially covered by mulches or row crops, a multidimensional description of upward flow in the soil is used [*Bristow and Horton*, 1996; *Horton*, 1989]. The few studies that also looked at heterogeneous flow and transport for upward directed flow (evaporation) reported conceptual problems with the definition of the boundary conditions at the soil surface [*Bechtold et al.*, 2012; *Schlüter et al.*, 2012].

Boundary conditions for the Richards equation are determined as a uniform flux boundary condition, which is derived by solving a surface energy balance, as long as a threshold pressure head is not reached. When the soil dries out and the critical pressure head is reached, the boundary condition is switched to a pressure head boundary condition. First, the definition of this critical pressure head is often debated. Second, for a heterogeneous soil surface in which patches of wet soil alternate with dried out areas, the evaporation rate from the wet patches may increase compared to the evaporation from a uniformly wet surface due to lateral exchange processes in the air flow (free flow) or in the porous medium. The effect of lateral exchange processes in the free flow on evaporation leads to the so-called ‘oasis effect’ and has been quantified to evaluate, for instance, the effect of the size of pores [*Assouline et al.*, 2010; *Shahraeeni and Or*, 2012], evaporation pans [*Brutsaert and Yu*, 1968], or ponds and lakes [*Harbeck*, 1962]. Lateral water and heat fluxes in heterogeneous porous media may lead to a larger water loss due to evaporation from a porous medium compared to the water loss from a homogeneous medium [*Lehmann and Or*, 2009; *Shahraeeni and Or*, 2011].

The general objective of this paper is to theoretically compare various model concepts used to describe evaporation processes from soils at the continuum scale. Modeling concepts vary in

complexity from fully coupled free flow and porous media flow representations to reduced complexity models such as those using Richards equations. First, we present the modeling concepts for flow and transport in the porous medium (i.e. soil), the free flow (i.e. atmosphere), and the coupling of the porous medium with the free flow (Figure 1). As different scientific communities (soil physics, hydrology, atmospheric sciences and micrometeorology, and fluid mechanics in porous media and in free flow) place different emphasis on the porous medium versus the free flow, oftentimes the coupling is strongly simplified or overlooked. This often leads to inconsistencies in the degree of detail with which processes are described in the porous medium or in the free flow (e.g. 3-D flow in the porous medium coupled with a 1-D transfer resistance to describe the exchange with the free flow) and misunderstandings between communities about the importance of different processes. Therefore, the first objective of this work is to present a comprehensive set of equations that describe all processes in both compartments (free flow and porous medium) and all relevant coupling conditions. This is followed a discussion of common by simplifications that lead to models of reduced complexity. Table 1, provides an overview of the constitutive equations for the two compartments, their interface and potential simplifications. What can be observed immediately from Table 1 is that the variables and parameters used in the various approaches differ significantly.

The second objective is to show the similarities and differences between the different approaches by deriving the variables and parameters based on a theoretical analysis of the comprehensive model. Model simplifications and 'fixes' are explained in detail, thus allowing for a full understanding of all approaches and for a classification of the simplifications.

In an accompanying paper, the consequences of these simplifications on the predictions of evaporation are investigated for two sets of exemplary simulations.

Coupled heat and water flow in porous media: overview of concepts and simplifications at the continuum scale

In this section, we introduce the model concepts used to describe heat and water fluxes in soils at the continuum scale. From the general balance equations, simplified equations are derived and the assumptions behind these simplifications are discussed. The employed constitutive equations are presented.

Balance equations:

A full description of water and vapor transport in a porous medium requires a description of flow of the two fluid phases, liquid and gas $\{l, g\}$, and of the transport of the components, water and dry air $\{w, a\}$ in each of the two phases. For simplicity, we consider air as a pseudo-component consisting of oxygen, nitrogen and other gases except vapor, which is regarded as separate component. A mass balance for each component $\kappa \in \{w, a\}$ is given by:

$$\sum_{\alpha \in (l,g)} \phi \frac{\partial \rho_\alpha X_\alpha^\kappa S_\alpha}{\partial t} + \nabla \cdot \boldsymbol{F}^\kappa = 0 \quad [1]$$

where ϕ is the porosity, which is assumed to be constant, ρ_α is the mass density of phase α [kg m^{-3}], X_α^κ is the mass fraction of component κ in phase α, S_α is the saturation or the volume fraction of the porosity occupied by phase α, $\mathbf{F}^\kappa$ is the mass flux of component κ [kg m^{-2} s^{-1}]. Source and sink terms (e.g. to account for liquid uptake by roots) are not included in the mass balance equations but can be simply added. The component mass flux $\mathbf{F}^\kappa$ is given by:

$$\boldsymbol{F}^\kappa = \sum_{\alpha \in (l,g)} \left(\boldsymbol{q}_\alpha \rho_\alpha X_\alpha^\kappa - D_{\alpha,pm}^\kappa \rho_\alpha \frac{M^\kappa}{\bar{M}_\alpha} \nabla x_\alpha^\kappa \right) \quad [2]$$

where $\mathbf{q}_\alpha$ [m s^{-1}] is the volume flux of phase α, $D^{\kappa}_{\alpha,pm}(S_\alpha)$ [m^2 s^{-1}] is the effective diffusion coefficient of component κ in phase α in the porous medium, x^{κ}_{α} is the molar fraction of κ in α, M^{κ} is the molar mass of κ and $\overline{M}_\alpha$ is the mole weighted average molar mass of phase α, with $\overline{M}_\alpha = x^{w}_{\alpha} M^{w} + x^{a}_{\alpha} M^{a}$. The effective diffusivity is lower than the diffusivity of κ in phase α alone: D^{κ}_{α} due to the tortuosity of the diffusive pathways and the smaller cross-sectional area available for diffusion within the porous medium, which depend both on the phase saturation [*Millington and Quirk*, 1961]. The volume fluxes are calculated with an extended Darcy's law for multiple fluid phases:

$$\boldsymbol{q}_\alpha = -\frac{k_{r\alpha}(S_\alpha)}{\mu_\alpha}\boldsymbol{k} \cdot \nabla(p_\alpha - \rho_\alpha \boldsymbol{g}\boldsymbol{z}) \quad [3]$$

where $k_{r\alpha}(S_\alpha)$ is the relative permeability of phase α at a saturation S_α, **k** is the intrinsic permeability tensor [m^2], μ_α [Pa s] is the dynamic viscosity of phase α, p_α [Pa] is the phase pressure, **g** [m s^{-2}] is the gravitational acceleration vector (directed downwards) and **z** [m] is the coordinate vector (positive upward). To close the system of equations, supplementary equations need to be specified.

First, the capillary pressure is defined as the pressure difference between the non-wetting and wetting phase: $p_c = p_g - p_l$. According to the Young-Laplace equation capillary pressure depends on the surface tension of the gas-fluid interface, σ(N m^{-1}), and on the curvature of the gas-liquid interfaces, *r* (m^{-1}), which depends on the saturation degree, S_l:

$$p_c = \frac{2\sigma(T)}{r(S_l)} \quad [4]$$

In continuum scale models, functional relations between the saturation degrees of the phases and the capillary pressure: $p_c = f(S_l)$, are used (e.g. [*Brooks and Corey*, 1964; *van Genuchten*, 1980]). Using simple pore network models, the form and parameters of relative permeability-saturation

functions were linked to the capillary pressure-saturation functions. In the Mualem van-Genuchten model, cylindrical pores are assumed. Assuming other pore geometries, e.g. triangular pores, lead to considerably higher permeabilities under dry soil conditions [*Diamantopoulos and Durner*, 2015; *Peters and Durner*, 2008; *Tuller and Or*, 2001]. Also, retention functions which describe the dry range of the water retention curve better than the van Genuchten function have been proposed and tested (e.g. [*Lu et al.*, 2008]) and might be more suited to describe evaporation processes.

Second, the sum of all phase saturations and of all mass fractions equals 1.

Third, a chemical equilibrium of a component between different phases may be assumed. This sets a relation between the mole fraction of air in the liquid phase, x_l^a, and the partial air pressure p_g^a [Pa] in the gas phase using Henry's law. Furthermore, a relation between the vapor pressure and the capillary pressure is given by Kelvin's equation [*Edlefsen and Anderson*, 1943]:

$$p_g^w = p_{g,sat}^w exp\left(-\frac{p_c M^w}{\rho_l RT}\right) \quad [5]$$

where $p_{g,\mathrm{sat}}^w$ [Pa] is the temperature-dependent saturated vapor pressure, $\mathrm{M^w}$ is the molecular weight of water [kg mol^{-1}], R is the universal gas constant [J mol^{-1} K^{-1}] and T [K] is the absolute temperature. The relation between the capillary pressure and the water vapor pressure only holds for dilute solutions. When the concentration of salts increases, also the osmotic soil water potential must be considered in Eq. [5] and an additional component equation for salt transport in the liquid phase and chemical equilibrium equations describing salt precipitation and dissolution must be included. We will not consider osmotic effects in the following but refer to [*Nassar and Horton*, 1997; 1999] who describe a model that considers coupled heat, vapor, liquid water, and solute transport. The mole fractions and partial pressures can be directly related to the mass fractions X_α^κ using molar weights and the ideal gas law:

$$\rho_g X_g^w = \rho_g^w = \frac{M^w p_g^w}{RT} = \frac{M^w p_{g,sat}^w}{RT} exp\left(-\frac{p_c M^w}{\rho_l RT}\right) \quad [6]$$

where ρ_g^w [kg m^{-3}] is the mass density of the vapor. The mole fraction of vapor in the gas phase can be calculated as:

$$x_g^w = \frac{p_g^w}{p_g} \quad [7]$$

When chemical equilibrium does not hold, extra equations to describe the mass exchange of components between different phases are required [*Benet and Jouanna*, 1982; *Chammari et al.*, 2008; *Nuske et al.*, 2014; *Ouedraogo et al.*, 2013; *Ruiz and Benet*, 2001; *Smits et al.*, 2011; *Trautz et al.*, 2015].

To properly approximate evaporative fluxes, it is important to account for the temperature conditions inside the porous medium. The vapor pressure and density of the air phase are two examples of temperature dependent state variables. A common assumption is that local thermal equilibrium between the gas, liquid and solid phase exists so that the temperatures in each of the three phases are equal to each other and a single energy balance equation can be used:

$$\sum_{\alpha\in\{l,g\}} \phi \frac{\partial \rho_\alpha u_\alpha S_\alpha}{\partial t} + (1-\phi)\frac{\partial \rho_s c_s T}{\partial t} + \nabla \cdot \boldsymbol{F}_T = 0 \quad [8]$$

where u_α [J kg^{-1}] is the internal energy of phase α, ρ_s [kg m^{-3}] is the mass density of the solid phase, c_s [J kg^{-1} T^{-1}] is the heat capacity of the solid phase, T [K] is the absolute temperature, and $\mathbf{F_T}$ [J m^{-2} s^{-1}] is the heat flux. The internal energy is related to the enthalpy, h_α [J kg^{-1}] plus the pressure-volume work:

$$u_\alpha = h_\alpha - \frac{p_\alpha}{\rho_\alpha} \quad [9]$$

The enthalpy of the liquid phase is usually assumed to be independent of composition. The gas phase enthalpy, h_g, is calculated from the mass fractions and component enthalpies, h^κ, of the dry air and water vapor components: $h_g = X_g^a h_g^a + X_g^w h_g^w$. Unlike the enthalpy of liquid water, the enthalpy of vapor also contains the latent heat of evaporation. The heat flux is described by:

$$\boldsymbol{F}_T = \sum_{\kappa\in\{a,w\}} \sum_{\alpha\in\{l,g\}} \left(\boldsymbol{q}_\alpha \rho_\alpha X_\alpha^\kappa - D_{\alpha,pm}^\kappa \rho_\alpha \frac{M^\kappa}{\bar{M}_\alpha} \nabla x_\alpha^\kappa \right) h_\alpha^\kappa - \lambda_{T,pm} \nabla T \qquad [10]$$

where $\lambda_{T,pm}$ [J m^{-1} s^{-1} K^{-1}] is the effective thermal conductivity under no mass flow conditions of the mixture of soil grains, liquid and gaseous phases. Mostly, relations are employed that derive $\lambda_{T,pm}$ from the volumetric liquid phase content. The parameters of these relations are a function of the texture of the porous medium, the organic matter content, and the dry bulk density [*Campbell*, 1985; *Chung and Horton*, 1987; *Cote and Konrad*, 2005; 2009; *de Vries*, 1963; *Lu et al.*, 2007; *Tarnawski et al.*, 2000]. Under some conditions with high fluid velocities, $\lambda_{T,pm}$ is also a function of the hydromechanical dispersion and heat capacity of the flowing fluid [*Campbell et al.*, 1994; *Hopmans et al.*, 2002].

Simplifications and fixes:

In this section, we describe ways to simplify the above derived equations and include additional processes that are not considered in the constitutive equations or simplified equations (e.g. chemical and thermal non-equilibrium and turbulence induced gas phase fluxes in the porous medium).

One component, 'one-and-a-half' phase equation:

In this approach, flow of the gas phase is not simulated but diffusive transport of components in the gas phase is still considered. Processes in the gas phase are thus considered 'half'.

This approach assumes that the pressure in the gas phase, p_g, is uniform and constant with time which results in the independence of the liquid phase pressure from flow in the gas phase. This assumption is justified based on the magnitude of the gas phase viscosity compared to that of the liquid phase (smaller by a factor 50). Therefore, Eq. [3] is only solved for the liquid phase and gas fluxes can be calculated directly from the change in the liquid phase saturation over time. Secondly, only the flux of the water component is considered, assuming that the water component flux is not influenced by the dry air concentrations in the two phases. For the liquid phase, this approximation hinges on the fact that the mass fraction of water in the liquid phase is close to one: $X_l^w \approx 1$. For the gas phase, the vapor pressure that is in equilibrium with the liquid phase is calculated from the capillary pressure (Eq. [5]), which depends only on the liquid phase pressure since the gas phase pressure is assumed to be constant. The vapor concentration is calculated using the ideal gas law (because $X_l^w \approx 1$) (Eq. [6]) and thus independent of the dry air concentration in the gas phase. Thirdly, it is assumed that advective fluxes of components in the gas phase can be neglected, $\boldsymbol{q_g}\rho_g X_g^w \approx 0$, compared with the diffusive fluxes. Finally, this approach assumes that gradients in the molar volume of the gas phase can be neglected and that the mass density of the liquid phase is constant. As a result of these assumptions, the water component flux equation (Eq. [2]) reduces to:

$$\boldsymbol{F}^w \approx \boldsymbol{q}_l\rho_l - \boldsymbol{D}_{g,pm}^w(S_g)\nabla\rho_g^w \qquad [11]$$

The mass balance equation for water simplifies to:

$$\phi\frac{\partial\rho_g X_g^w S_g}{\partial t} + \phi\frac{\partial\rho_l S_l}{\partial t} - \nabla\cdot\left[\frac{\rho_l k_{rl}(S_l)}{\mu_l}\boldsymbol{k}\nabla(p_l - \rho_l\boldsymbol{g}\boldsymbol{z})\right] - \nabla\cdot\left[\boldsymbol{D}_{g,pm}^w\nabla\rho_g^w\right] = 0 \qquad [12]$$

This is the basic equation used by the soil physics community to describe non-isothermal liquid water flow and water vapor transport in soils. However, it is usually expressed in the following form [*Milly*, 1982; *Saito et al.*, 2006]:

$$\frac{\partial \theta_l}{\partial t} + \frac{\partial \theta_v}{\partial t} = \nabla \cdot \left[\left(\boldsymbol{K}_{l,\psi} + \boldsymbol{K}_{v,\psi} \right) \frac{\sigma(T)}{\sigma\left(T_{ref}\right)} \nabla \psi|_{Tref} + \boldsymbol{K}_{l,\psi} \boldsymbol{e_z} \right] + \nabla \cdot \left(\boldsymbol{K}_{l,T} + \boldsymbol{K}_{v,T} \right) \nabla T \quad [13]$$

where $\theta_l = \phi S_l$ is volumetric liquid water content and θ_v the water vapor content expressed in volume of liquid water ($\theta_v = \phi \rho_g^w S_g / \rho_l$), $\mathbf{K}_{l,x}$ and $\mathbf{K}_{v,x}$ are the hydraulic conductivities for liquid water flow and vapor transport, respectively, $\mathbf{K}_{x,\psi}$ [m s^{-1}] and $\mathbf{K}_{x,T}$ [m^2 K^{-1} s^{-1}] are the isothermal and thermal hydraulic conductivities, respectively, $\boldsymbol{e_z}$ is the unit coordinate vector in the vertical direction, and $\psi|_{Tref}$ (m) is the pressure head of the liquid phase at the reference temperature T_{ref}. The first term on the right hand side of Eq. [13] represents the total water flow due to pressure head gradients under isothermal conditions and due to gravity. Since the pressure head gradients are defined at a reference temperature, a standard relation between θ_l and $\psi|_{Tref}$ can be used. The second term on the right hand side accounts for the total water fluxes that are generated by a thermal gradient.

In the following section, the relationships between the hydraulic properties $\mathbf{K}_{xy}$, the variables θ_v, θ_l, $\psi|_{Tref}$, and T, the fluid properties, and the effective diffusion coefficients and permeability are presented and the equality between Eqs. [12] and [13] elucidated.

The pressure head ψ of the water phase can be defined in terms of the capillary pressure p_c as:

$$p_c = -\psi g \rho_l \quad [14]$$

Assuming a uniform and constant gas phase pressure and liquid phase density, the water pressure gradient can be replaced by the pressure head gradient multiplied by a constant factor $g\rho_l$. Considering Eq. [4] the spatial gradient of ψ can be written as:

$$\nabla \psi(\theta_l, T) = \left. \frac{\partial \psi}{\partial \theta_l} \right|_T \nabla \theta_l + \left. \frac{\partial \psi}{\partial \sigma} \right|_{\theta_l} \frac{\partial \sigma}{\partial T} \nabla T \quad [15]$$

or

$$\nabla\psi(\theta_l,T)=\left.\frac{\partial\psi}{\partial\theta_l}\right|_T\nabla\theta_l+\left.\frac{\psi}{\sigma}\right|_{\theta_l}\frac{\partial\sigma}{\partial T}\nabla T \quad [16]$$

$$\nabla\psi(\theta_l,T)=\left.\frac{\partial\psi}{\partial\theta_l}\right|_T\left.\frac{\partial\theta_l}{\partial\psi}\right|_{Tref}\nabla\psi|_{Tref}+\left.\frac{\psi_{Tref}}{\sigma(T_{ref})}\right|_{\theta_l}\frac{\partial\sigma}{\partial T}\nabla T \quad [17]$$

$$\nabla\psi(\theta_l,T)=\frac{\sigma(T)}{\sigma(T_{ref})}\nabla\psi|_{Tref}+\left.\frac{\psi_{Tref}}{\sigma(T_{ref})}\right|_{\theta_l}\frac{\partial\sigma}{\partial T}\nabla T \quad [18]$$

The first term of the right hand side of Eq. [16] represents the gradient in pressure head due to a gradient in the volumetric water content under isothermal conditions. Using the relationship between pressure head and volumetric water content at a reference temperature, T_{ref}, this term can be rewritten in terms of a pressure head gradient at a reference temperature (first term of Eq. [18]). The second term in Eq. [16] represents the gradient in pressure head due to a temperature gradient at a given volumetric water content θ_l. This term can also be rewritten in terms of a pressure head for a given water content θ_l at a reference temperature (Eq. [18]).

In a similar vein, the gradient $\nabla\rho_g^w$ can be written as:

$$\nabla\rho_g^w(\psi,T)=\left.\frac{\partial\rho_g^w}{\partial\psi}\right|_T\frac{\sigma(T)}{\sigma(T_{ref})}\nabla\psi|_{Tref}+\left.\frac{\partial\rho_g^w}{\partial T}\right|_\psi\nabla T \quad [19]$$

Including Equations [14], [18], and [19] in Eq. [12] leads to the following equation:

$$\frac{\partial\theta_v}{\partial t}+\frac{\partial\theta_l}{\partial t}=\nabla\cdot\left[\left(\boldsymbol{K}_{l,\psi}+\frac{\boldsymbol{D}_{g,pm}^w(S_g)}{\rho_l}\left.\frac{\partial\rho_g^w}{\partial\psi}\right|_T\right)\frac{\sigma(T)}{\sigma(T_{ref})}\nabla\psi|_{Tref}+\boldsymbol{K}_{l,\psi}\boldsymbol{e_z}\right] \quad [20]$$

$$+\nabla\cdot\left[\left(\boldsymbol{K}_{l,\psi}\left.\frac{\psi_{Tref}}{\sigma(T_{ref})}\right|_{\theta_j}\frac{\partial\sigma}{\partial T}+\frac{\boldsymbol{D}_{g,pm}^w(S_g)}{\rho_l}\left.\frac{\partial\rho_g^w}{\partial T}\right|_\psi\right)\nabla T\right]$$

Using the relation between the vapor density, capillary pressure and temperature (Eq. [6]) and defining the saturated vapor density $\rho_{g,sat}^w$ [kg m^{-3}] and the relative humidity of the air $H_r = \rho_g^w/\rho_{g,sat}^w$ it follows from Eq. [20] that the conductivities in Eq. [13] are defined as:

$$\boldsymbol{K}_{l,\psi} = \frac{\rho_l g k_{rl}(S_l)}{\mu_l}\boldsymbol{k} \quad [21]$$

$$\boldsymbol{K}_{v,\psi} = \frac{g M_w \rho^w_{g,sat} H_r}{\rho_l RT}\boldsymbol{D}^w_{g,pm}(S_g) \quad [22]$$

$$\boldsymbol{K}_{l,T} = \boldsymbol{K}\frac{\psi_{Tref}}{\sigma(T_{ref})}\Big|_{\theta_l}\frac{\partial\sigma}{\partial T} \quad [23]$$

$$\boldsymbol{K}_{v,T} = \frac{H_r}{\rho_l}\frac{\partial\rho^w_{g,sat}}{\partial T}\boldsymbol{D}^w_{g,pm}(S_g) \quad [24]$$

Eq. [13] relies on the assumption of local thermal equilibrium. However, the temperature of the air, water and soil particles may differ due to the difference in thermal properties of these phases and rapid changes of soil surface temperatures. Therefore, it is argued that the temperature gradient in the soil air is often larger than the gradient of the mean temperature over the different phases. The effective diffusion of water vapor in soil may be larger than that of other gases since water vapor may condense and evaporate from capillary held water pockets (i.e. "liquid bridges" or "capillary islands"), thus blocking the diffusive transport of other gases [*Philip and De Vries*, 1957]. These effects have been used to explain observations of enhanced vapor transport compared to Fick's law of diffusion [*Gurr et al.*, 1952; *Rollins et al.*, 1954; *Taylor and Cavazza*, 1954]. To account for this, $K_{v,T}$ is multiplied by an enhancement factor η [*de Vries*, 1958; *Philip and De Vries*, 1957] described by empirical formulations (e.g. [*Campbell*, 1985; *Cass et al.*, 1984]). This approach has been widely used and accepted to calculate heat and water flow in soils (e.g. [*Hadas*, 1977; *Reshetin and Orlov*, 1998; *Rose*, 1967; *Shepherd and Wiltshire*, 1995; *Sophocleous*, 1979]). However, the validity or need for vapor enhancement has been questioned [*Ho and Webb*, 1998; *Shokri et al.*, 2009; *Smits et al.*, 2013].

In addition ot vapor enhancement, an enhancement of the liquid flow that is induced by thermal gradients has been proposed [*Noborio et al.*, 1996; *Saito et al.*, 2006]. This enhancement is attributed to the change in surface tension that results from changes in soil water composition

(ionic strength, concentration of organic surfactants) with temperature. Thermal enhancement is accounted for by multiplying $K_{l,T}$ (Eq. [23]) by a non-dimensional empirical 'gain factor' ranging in value from 0 to 10 [*Nimmo and Miller*, 1986].

In Eqs. [18] and [19], the gradients in the pressure head and vapor mass density were written in terms of gradients in temperature and pressure head at a reference temperature assuming that the change in water content with pressure head, $\frac{\partial \theta_l}{\partial \psi}$, is only a function of the surface tension, σ, and temperature effects were attributed to changes in σ with temperature. But, the relationship between θ_l and ψ also depends on the interaction between the solid and liquid phase (i.e. the contact angle between the liquid-gas surface and the solid phase or solid phase wettability) which may also change with temperature [*Bachmann et al.*, 2002]. Therefore, it is important to note that for non-wettable soils temperature effects on solid-liquid phase interactions should be included in the model to predict reduced evaporation from non-wettable soils or reduced water redistribution due to temperature gradients in non wettable soil [*Bachmann et al.*, 2001; *Davis et al.*, 2014].

Isothermal one component, 'one-and-a-half' phase equation:

When water fluxes are considered over a longer period of time (i.e. multiple days), it may be argued that the temporal average of the temperature gradients cancels out due to diurnal variations in temperature. This also results in the temperature gradient driven fluxes canceling out [*Milly*, 1984]. Based on this assumption, the flow equation can be simplified to an isothermal equation and flow due to a temperature gradient (i.e. in Eq. [13]) can be neglected so that for a 1-D flow process (as routinely assumed in soils), the following equation is obtained:

$$\frac{\partial \theta_v}{\partial t} + \frac{\partial \theta_l}{\partial t} = \frac{\partial}{\partial z} \cdot \left[\left(K_{l,\psi} + K_{v,\psi} \right) \frac{\partial \psi}{\partial z} + K_{l,\psi} \right] \quad [25]$$

Isothermal one component one phase equation, Richards equation

Finally, when vapor transport is neglected, the classical Richards equation is obtained:

$$\frac{\partial \theta_l}{\partial t} = \frac{\partial}{\partial z} \cdot \left[K_{l,\psi} \frac{\partial \psi}{\partial z} + K_{l,\psi} \right] \quad [26]$$

Flow and transport processes in the atmosphere

In this section, the free flow balance equations are described and then possible simplifications are presented and discussed.

Balance equations

In the context of evaporation processes from soils, flow conditions in the free flow are mostly turbulent. Turbulent flow is usually highly irregular with chaotic fluctuations of the local velocity, pressure, concentration and temperature [*Bird et al.*, 2007]. These fluctuations are caused by vortices or eddies, which occur over a wide range of length scales. It is possible to simulate all of these phenomena, but it requires the resolution of eddies on all scales and has therefore high computational costs. To reduce these costs, turbulence can be parameterized rather than simulated explicitly. The most commonly used parametrization approach is the so-called Reynolds averaging. The basic assumption is that turbulent fluctuating quantities can be split in a temporal average $\overline{v}$ and a fluctuating part v'. This is called the Reynolds decomposition:

$$v_g = \overline{v}_g + v'_g, \quad p_g = \overline{p}_g + p'_g, \quad x_g^\kappa = \overline{x_g^\kappa} + x_g^{\kappa\prime}, \quad T = \overline{T} + T' \quad [27]$$

where v_g [m s^{-1}] is the gas velocity.

After replacing the instantaneous values in the balance equations by the sum of the average and fluctuating parts, the balance equations are averaged over time. For a more detailed overview on turbulence modeling and the Reynolds averaging procedure, we refer the reader to standard fluid dynamic textbooks (e.g. [*Bird et al.*, 2007; *Wilcox*, 2006]). The total mass balance for the gas phase is:

$$\frac{\partial \rho_g}{\partial t} + \nabla \cdot \left[\rho_g \, \overline{\boldsymbol{v}_g}\right] = 0 \qquad [28]$$

408 The momentum balance is:

$$\frac{\partial (\rho_g \overline{\boldsymbol{v}_g})}{\partial t} + \nabla \cdot \left[\rho_g \, \overline{\boldsymbol{v}_g} \, \overline{\boldsymbol{v}_g} + \underbrace{\rho_g \boldsymbol{v}_g{}' \boldsymbol{v}_g{}'}_{\substack{turbulent\ stress/ \\ Reynolds\ stress}} + \overline{p_g} \boldsymbol{I} - \overline{\boldsymbol{\tau}}_g \right] - \rho_g \boldsymbol{g} = 0 \qquad [29]$$

409 The gas phase is considered to act as a Newtonian fluid without dilatation, therefore the shear
410 stress tensor $\boldsymbol{\tau}_g$ [kg m^{-1} s^{-2}] solely accounts for the resistance to shear deformation:

$$\boldsymbol{\tau_g} = \mu_g \left(\nabla \overline{\boldsymbol{v_g}} + \nabla \overline{\boldsymbol{v_g}}^{\boldsymbol{T}} \right) \qquad [30]$$

411 where μ_g [kg s^{-1} m^{-1}] is the dynamic viscosity of the gas phase.

412 The component mass balance is given by:

$$\frac{\partial \rho_g \overline{X_g^\kappa}}{\partial t} + \nabla \cdot \left(\rho_g \, \overline{\boldsymbol{v}_g} \overline{X_g^\kappa} + \underbrace{\rho_g \, \boldsymbol{v}_g{}' X_g^{\kappa\prime}}_{turbulent\ diffusion} - D_g^\kappa \, \rho_g \frac{M^\kappa}{\overline{M_g}} \nabla \overline{x_g^\kappa} \right) = 0 \qquad [31]$$

413 and the energy balance by:

$$\frac{\partial \rho_g \, \overline{u_g}}{\partial t} + \nabla \cdot \left(\rho_g \, \overline{\boldsymbol{v}_g} \, \overline{h_g} + \underbrace{\rho_g \, \boldsymbol{v}_g{}' \, h_g{}'}_{turbulent\ conduction} - \lambda_{T,g} \nabla \overline{T} - \sum_{\kappa \in \{a,w\}} h_g^\kappa D_g^{\kappa,} \rho_g \frac{M^\kappa}{\overline{M_g}} \nabla \overline{x_g^\kappa} \right) = 0 \qquad [32]$$

414

415 Multiplication of the turbulent fluctuations in the abovementioned balance equations (e.g. the
416 convective portion of the momentum balance equation) leads to additional terms. Physically-
417 speaking, these terms, although originating from the convective portion of the equation, act like
418 additional viscous, diffusive, and conductive forces. Therefore, they are referred to as turbulent
419 stress, turbulent diffusion, or turbulent conduction and require parameterization to properly
420 account for the effects of turbulence. Various parameterizations of different complexity are well-
421 established in literature. The simplest one is based on the Boussinesq assumption [*Boussinesq*,
422 1872] which states that the Reynolds stress acts completely like a viscous stress so that only one
423 unknown per balance equation remains. These unknowns are called eddy coefficients: eddy

viscosity μ_g^{turb} [kg m^{-1} s^{-1}], eddy diffusivity D_g^{turb} [m^2 s^{-1}], and eddy conductivity λ_g^{turb} [W m^{-1} K^{-1}] [*Wilcox*, 2006]. The most fundamental approach for calculating the eddy viscosity is based on the Prandtl mixing length:

$$-\rho_g \boldsymbol{v}'_g \boldsymbol{v}'_g = \boldsymbol{\tau}_g^{turb} = \mu_g^{turb}\left(\nabla \overline{\boldsymbol{v}}_{\boldsymbol{g}} + \nabla \overline{\boldsymbol{v}}_{\boldsymbol{g}}^{\boldsymbol{T}}\right)$$
$$\mu_g^{turb} = \rho_g \, l_{mix}^2 \left|\frac{\partial \overline{v_x}}{\partial z}\right| \quad [33]$$

where $l_{mix} = \kappa z$ is the mixing length [m], κ is the von-Karman constant [-], z is the wall distance [m], and v_x the main velocity component [m s^{-1}]. The dynamic eddy viscosity can be converted to the kinematic eddy viscosity with:

$$\nu_g^{turb} = \frac{\mu_g^{turb}}{\rho_g} = l_{mix}^2 \left|\frac{\partial \overline{v_x}}{\partial z}\right| \quad [34]$$

In this model the kinematic eddy viscosity, ν_g^{turb}, is only a function of the flow and its turbulence, not of the fluid type itself.

In addition to the eddy viscosity, the eddy diffusivity and conductivity still need to be resolved. The most pragmatic approach is by applying the Reynolds analogy. It assumes that the same mechanisms leading to the eddy viscosity also lead to a higher mixing rate. Then the eddy diffusivity is related to the eddy viscosity by the turbulent Schmidt number:

$$D_g^{\kappa,turb} = \frac{\mu_g^{turb}}{\rho_g \, Sc^{turb}} \quad [35]$$

In the same way the eddy conductivity is obtained with the turbulent Prandtl number:

$$\lambda_{T,g}^{turb} = \frac{c_p \, \mu_g^{turb}}{Pr^{turb}} \quad [36]$$

The turbulent Schmidt and Prandtl numbers are often assumed to be one.

Simplifications

The solution of the three-dimensional balance equations in the free flow is computationally demanding. To simplify the solution, it is often assumed that the mean wind speed, air temperature, and relative humidity (i.e. vapor content of the air) do not change in the horizontal direction or along the air stream and that their changes over time are slow. This assumption implies that the momentum, vapor, and sensible heat fluxes out of the soil surface are equal to the respective fluxes in the vertical direction in the air stream above the soil surface and do not change with height. This generally applies for a sufficiently large upstream fetch of a homogeneous evaporating surface (no lateral variations in soil water content, soil temperature, evaporation fluxes, and soil surface roughness). It also implies that the vertical component of the air flow is assumed to be zero in both the porous medium and the free flow, which is consistent with the one component 'one-and-a-half' phase formulation of the flow and transport process in the porous medium.

When the momentum transfer occurs mainly through turbulent eddies, of which the size increases linearly with height, the eddy viscosity increases linearly with height so that the turbulent shear stress τ_{turb} is given by:

$$\tau_{turb} = \rho_g \kappa v^* z \frac{dv_x}{dz} \quad [37]$$

where v^* [m s^{-1}] is the friction velocity and κ is the von Karman constant (≈ 0.4). It should be noted that $\rho_g \kappa v^* z$ corresponds with the turbulent viscosity μ_g^{turb} in Eq. [33]. This leads to logarithmic wind profiles that are generally observed in the so-called turbulent or 'dynamic' sublayer:

$$v_x\ (z) = \frac{v^*}{\kappa} ln\left(\frac{z}{z_{0\mathrm{m}}}\right) \quad [38]$$

where z_{0m} [m] is the momentum roughness length, which corresponds to the height above the soil surface where extrapolation of Eq. [38] predicts zero velocity. Similar logarithmic profiles are obtained for the air temperature and humidity. But, because of different interactions at the soil surface, the temperature (z_{0H}) and humidity (z_{0v}) roughness lengths differ from z_{0m}. The relationship between the different roughness lengths and characteristics of the porous medium-free flow interface are discussed in the following section.

Heat and water fluxes across the soil-atmosphere interface

The soil-atmosphere interface represents a crucial boundary between the porous medium and the free flow. In this section the coupling between transport in the atmosphere and the soil is discussed.

Coupling conditions:

The coupling of the two-phase porous-medium system with turbulent free flow involving the Reynolds-averaged Navier-Stokes equations is based on the model presented in *Mosthaf et al.* [2011] and revised in *Mosthaf et al.* [2014] and *Fetzer et al.* [2016]. It considers continuity of fluxes and a local thermodynamic equilibrium at the interface.

Mechanical equilibrium

Mechanical equilibrium is defined by the continuity of normal and tangential forces. The normal force acting on the interface from the free flow side is the sum of the inertia, pressure, and viscous forces. The normal force from the porous-medium side of the interface contains only the pressure force, since viscous forces are implicitly accounted for in Darcy's law. Hence, the mechanical equilibrium at the interface in the normal direction can be formulated as:

$$\left[\boldsymbol{n} \cdot \left(\{-\rho_g \, \boldsymbol{v}_g \, \boldsymbol{v}_g \, - \boldsymbol{\tau}_g \, - \boldsymbol{\tau}_g^{turb} + p_g \boldsymbol{I}\}\boldsymbol{n}\right)\right]^{ff} = \left[p_g\right]^{pm} \qquad [39]$$

The superscripts ff and pm mark the quantities at the free flow and the porous medium sides of the interface in the sequel. Eq. [39] implies that the gas phase pressure may be discontinuous across the interface due to the different model concepts (i.e. Navier-Stokes flow and Darcy flow) in the two domains. Furthermore, in addition to considering the normal forces, the free flow requires a condition for the tangential flow velocity components. When air flows over a porous surface, there is a small macroscopic slip-velocity, which therefore calls the no-slip condition into question. For that purpose, the Beavers-Joseph [*Beavers and Joseph*, 1967] or Beavers-Joseph-Saffman [*Saffman*, 1971] condition can be employed; the latter formulation neglects the comparatively small tangential velocity in the porous medium. The proportionality between the shear stresses τ and the slip velocity at the interface can be described as:

$$\left[\left(\boldsymbol{v}_g - \frac{\sqrt{k_i}}{\alpha_{BJ}\mu_g}\left(\boldsymbol{\tau}_g + \boldsymbol{\tau}_g^{turb}\right)\boldsymbol{n}\right)\cdot \boldsymbol{t}_i\right]^{ff} = 0, \quad i \in \{1, \dots, d-1\} \qquad [40]$$

Here, α_{BJ} is the dimensionless Beavers-Joseph coefficient, $\boldsymbol{t}_i$ is a tangential vector, and $k_i = \boldsymbol{t}_i \cdot (k\boldsymbol{t}_i)$ a tangential component of the permeability tensor. The Beavers-Joseph condition was originally developed for flow which is mainly tangential to the porous-medium surface and for laminar single-phase flow in both the free flow and the porous medium. Its applicability for turbulent flow conditions was analyzed by *Hahn et al.* [2002] who concluded that the slip condition for laminar and turbulent flow is the same, because the flow conditions directly at the porous surface can be expected to be laminar (viscous boundary layer) and velocities to be slow.

The influence of the Beavers-Joseph coefficient on the evaporation rate was analyzed in various studies for different flow regimes [*Baber et al.*, 2012; *Fetzer et al.*, 2016]. For flow parallel to the interface the evaporative fluxes are often dominated by diffusion through the boundary layer normal to the interface [*Haghighi et al.*, 2013], whereas the slip velocity promotes transport along the interface.

Chemical equilibrium

Ideally, chemical equilibrium should be formulated as continuity of the chemical potential. The problem is that the assumption of mechanical equilibrium, as previously discussed, leads to a jump in gas phase pressure across the interface. This jump in gas phase pressure comes along with a jump in vapor pressure across the interface and consequently a jump in chemical potential. Hence, continuity cannot be expressed in terms of chemical potentials. Instead, it is expressed in terms of the continuity of mole fractions in the gas phase.

The continuity of component fluxes is given by:

$$\left[\left(\rho_g \boldsymbol{v}_g X_g^\kappa - \left(D_g + D_g^{turb}\right)\rho_g \frac{M^\kappa}{\overline{M}_g}\nabla x_g^\kappa\right)\cdot \boldsymbol{n}\right]^{ff} = -\left[\left(\rho_g \boldsymbol{q}_g X_g^\kappa - D_{g,pm}^\kappa \rho_g \frac{M^\kappa}{\overline{M}_g}\nabla x_g^\kappa + \rho_l \boldsymbol{q}_l X_l^\kappa - D_{l,pm}^\kappa \rho_l \frac{M^\kappa}{\overline{M}_l}\nabla x_l^\kappa\right)\cdot \boldsymbol{n}\right]^{pm} \quad [41]$$

The minus sign in the flux continuity accounts for the opposed directions of the normal vector of the porous medium and the free flow domain (see Figure 1). When summing up the two components, the continuity of total mass flux is given by:

$$\left[\rho_g \boldsymbol{v}_g \cdot \boldsymbol{n}\right]^{ff} = -\left[\left(\rho_g \boldsymbol{q}_g + \rho_l \boldsymbol{q}_l\right)\cdot \boldsymbol{n}\right]^{pm} \quad [42]$$

Thermal equilibrium

Thermal equilibrium assumes continuity of temperature at the interface. The free flow temperature is equal to the temperature of the gas phase; in contrast, the porous medium temperature is the temperature of one REV under the assumption of local thermal equilibrium.

The continuity of heat fluxes is given by:

$$\left[\left(\rho_g h_g \boldsymbol{v}_g - \left(\lambda_{T,g} + \lambda_{T,g}^{turb}\right)\nabla T - \sum_{\kappa\in\{a,w\}} h_g^\kappa \left(D_g^\kappa + D_g^{turb}\right)\rho_g \frac{M^\kappa}{\overline{M}} \nabla x_g^\kappa\right)\cdot \boldsymbol{n}\right]^{ff} = \quad [43]$$

$$R_n - \left[\left(\sum_{\kappa\in\{a,w\}}\sum_{\alpha\in\{l,g\}} \left(\boldsymbol{q}_\alpha \rho_\alpha X_\alpha^\kappa - D_{\alpha,pm}^\kappa \rho_\alpha \frac{M^\kappa}{\overline{M}_\alpha}\nabla x_\alpha^\kappa\right) h_\alpha^\kappa - \lambda_{T,pm}\nabla T\right)\cdot \boldsymbol{n}\right]^{pm}$$

The coupling condition for the energy balances may also include the net radiation R_n [J m^{-2} s^{-1}] as an additional energy flux to the porous medium. However, the assumption of thermal equilibrium may be violated in case of fast invasion of water with a different temperature or strong temperature differences between the free flow and porous medium [*Nuske et al.*, 2014].

Simplifications and fixes:

The exchange processes are closely linked to the geometry and the roughness of the interface which is not resolved in the abovementioned simulation models. The effect of this non-resolved geometry or roughness needs to be parameterized in the coupling conditions. In the following section, we discuss several simplifications that are made for coupling processes in the porous medium and the free flow.

Full turbulence model and roughness

For smooth surfaces, the effects of turbulence inside the viscous boundary layer are negligible. Therefore, the eddy coefficients approach zero and are not necessarily required in the coupling conditions.

For smooth surfaces, the roughness elements are covered with a viscous boundary layer, although the flow above the viscous layer may be turbulent. In this case the roughness influences the profile

549 of the eddy coefficients in the direction normal to the surface and thus the velocity profile and the
550 viscous boundary layer thickness. Still, the coupling occurs in the viscous boundary layer.
551 For rough surfaces, the height of the roughness elements is larger than the viscous layer thickness
552 and the effects of the roughness and turbulence are important and cannot be neglected [*Fetzer et*
553 *al.*, 2016]. This is accomplished by including the eddy coefficients, which are a function of
554 roughness, in the coupling conditions above. In the section on one-dimensional transfer between
555 the porous medium and the free flow, more details on the effect of roughness on the exchange
556 processes are given.
557

558 **Coupled one-dimensional transfer between the soil surface and free flow: aerodynamic**
559 **resistances.**

560 When lateral variations in wind, air temperature and humidity can be neglected, the sensible heat
561 and vapor fluxes can be described as one-dimensional fluxes that are calculated using equivalent
562 transfer resistances and differences in vapor concentrations and temperature that are measured at
563 different heights but at the same horizontal location (e.g. [*Monteith and Unsworth*, 1990]):

$$H = c_a \frac{T(z=0) - T(z_{ref})}{r_H} \quad [44]$$

$$F_w = \frac{\rho_g^w(z=0) - \rho_g^w(z_{ref})}{r_V} \quad [45]$$

564

565 where H [J m^{-2} s^{-1}] is the sensible heat flux, c_a [J m^{-3} K^{-1}] is the volumetric heat capacity of moist
566 air, z_{ref} (m) is a reference height at which wind speed, air temperature and air humidity are
567 measured or defined, F_w [kg m^{-2} s^{-1}] is the water vapor flux, and r_H and r_V [s m^{-1}] are the
568 aerodynamic resistance terms for vertical latent heat and vapor transfer in the air stream. Using a
569 mass and energy balance at the soil surface, the vapor and sensible heat fluxes are linked to the
570 water and vapor fluxes in the soil at the soil surface. The mass balance is given by:

$$F_w = \left[q_l \rho_l - D_{g,eff}^w(S_g) \frac{\partial \rho_g^w}{\partial z} \right]^{pm} \quad [46]$$

571

572 where the first and second terms on the right hand side are the liquid water and vapor flows towards
573 the soil surface, respectively.

574 For the energy balance equation at the soil surface, the solar and long wave radiation that is
575 absorbed by and emitted from the soil surface needs to be taken into account. Calling the sum of
576 these radiation terms the net radiation, R_n [J m^{-2} s^{-1}] (where positive radiation terms denote the
577 radiation that is absorbed and negative terms denote the radiation that is emitted), the energy
578 balance at the soil surface is:

$$H + h_g^w F_w - R_n = \left[-h_g^w D_{g,eff}^w(S_g) \frac{\partial \rho_g^w}{\partial z} + h_l^w \rho_l q_l - \lambda_{T,pm} \frac{\partial T}{\partial z} \right]^{pm} \quad [47]$$

579

580 Eqs. [44], [45], [46], [47] link the state variables, i.e. temperature and air vapor concentration, and
581 fluxes at the soil surface with state variables that are defined at the reference height in the air
582 stream. The latter may therefore be considered as Dirichlet boundary conditions for the water and
583 heat fluxes in the coupled soil-air system. This implies that the water and heat fluxes at the soil
584 surface can be derived from these prescribed state variables in the air stream and do not have to be
585 prescribed as flux boundary conditions.

586

587 Crucial parameters in Eqs. [44] and [45] are the aerodynamic resistance terms for vertical latent
588 and sensible heat transfer. They are related to the roughness of the soil surface, diffusive transfer
589 in the interfacial viscous or roughness layer, wind velocity and eddy diffusivity in the air stream,
590 and stability of the air above the heated soil surface. In the following discussion, we will consider
591 neutral stability conditions, i.e. the eddy diffusivity is not influenced by buoyancy. We refer the

reader to text books on meteorology (e.g. [*Brutsaert*, 1982; *Monteith and Unsworth*, 1990; *Shuttleworth*, 2012]) for a detailed treatment of buoyancy effects.

In the air stream, a constant shear stress, τ_{turb} [N m^{-2}], with height is assumed. τ_{turb} corresponds to a momentum transfer from the air stream to the soil surface and can be expressed in terms of a resistance equation similar to Eqs. [44] and [45]:

$$\tau_{turb} = \rho_g \frac{v_{g,x}(z_{ref}) - v_{g,x}(z=0)}{r_M} \quad [48]$$

where $v_{g,x}$[m s^{-1}] is the horizontal air velocity, and r_M [s m^{-1}] is the resistance for momentum transfer between the reference height and the soil surface. r_M is derived from the vertical wind profile in the 'logarithmic/dynamic' sublayer above the roughness layer.

Combining Eqs. [37], [38], and [48] leads to the following expression for r_M:

$$r_M = \frac{ln\left(\frac{z}{z_{0\mathrm{m}}}\right)}{v^*\kappa} = \frac{\left\{ln\left(\frac{z}{z_{0\mathrm{m}}}\right)\right\}^2}{v_{g,x}(z)\kappa^2} \quad [49]$$

The momentum roughness length, z_{0m}, is a function of the kinematic viscosity of air, ν, the friction velocity, v^*, and the height and density of the roughness elements of the soil surface. For rough surfaces z_{0m} depends only on the roughness of the surface. A prediction of z_{0m} based on the geometry of the surface roughness seems to be very uncertain and *Wieringa* [1993] found that the relationship between z_{0m} and the height of the surface roughness elements, *d*, may vary between:

$$z_{0\mathrm{m}} = \frac{d}{100} \quad and \quad z_{0\mathrm{m}} = \frac{d}{5} \quad [50]$$

For a small *d* or smooth surfaces, a viscous sublayer in which momentum transfer is dominated by kinematic viscosity develops. In such a case, the velocity profiles and z_{0m} depend on v^* and ν:

$$z_{0m} = 0.135\frac{\nu}{v^*} \quad [51]$$

611

612 Whether a surface is rough or (hydrodynamically) smooth depends on the roughness Reynolds
613 number, z_{0+} which is defined as:

$$z_{0+} = \frac{v^* z_{0\mathrm{m}}}{\nu} \quad [52]$$

614

615 When $z_{0+} > 2$, the surface is considered to be rough whereas z_{0+} equals 0.135 for flat surfaces. It
616 should be noted that when z_{0m} is defined by *d*/30, the following well-known relation for a wind
617 speed profile above a rough surface is obtained [*White*, 1991]:

$$v_x(z) = \frac{v^*}{\kappa} ln\left(\frac{z}{d}\right) + 8.5v^* \quad [53]$$

618

619 For smooth surfaces, the following relation is obtained:

$$v_x(z) = \frac{v^*}{\kappa} ln\left(\frac{zv^*}{\nu}\right) + 5.0v^* \quad [54]$$

620

621 The transfer of water vapor and sensible heat in the logarithmic/dynamic sublayer is also caused
622 by turbulence and eddy diffusivity, which according to the Reynolds analogy may be considered
623 equivalent to the eddy viscosity. Therefore, a close relation between the transfer resistances for
624 momentum, sensible heat and vapor transfer may be assumed. Yet, these resistances differ from
625 each other because of the different transfer mechanisms in the viscous or roughness layer. The
626 kinematic air viscosity differs from the molecular diffusion of water and heat. Also, the roughness
627 of a bluff surface has a different effect on momentum transfer than on transfer of a scalar quantity
628 like vapor or sensible heat. For rough surfaces, momentum transfer can be considered more
629 effective or influential than vapor or heat transfer. Therefore the resistance for heat/vapor transfer
630 is larger than that for momentum transfer. As a consequence, an additional boundary resistance,

631 r_B [s m^{-1}] must be considered when relating the transfer resistances for vapor and sensible heat
632 transfer to the momentum transfer:

$$r_V \approx r_H = r_M + r_B \quad [55]$$

633

634 The larger resistance results in a larger gradient of vapor and temperature across the viscous or
635 roughness layer; the vapor and heat roughness lengths z_{0v} and z_{0H} are therefore smaller than z_{0m}.
636 The similar transfer through the logarithmic/dynamic layer allows for the transfer resistance for
637 vapor and heat transport to be described using an equation similar to Eq. [49]:

$$r_{V,H} = \frac{ln\left(\frac{z}{z_{0\,v,H}}\right)}{v^*\kappa} = \frac{\left\{ln\left(\frac{z}{z_{0\,v,H}}\right)\right\}^2}{v_{g,x}(z)\kappa^2} \quad [56]$$

638

639 This equation may be rewritten in terms of r_m and r_B as:

$$r_{V,H} = r_M + r_B = \frac{ln\left[\frac{z}{z_{0\,V,H}}\right]}{\kappa v^*} = \frac{ln\left[\frac{z}{z_{0\mathrm{m}}}\right]}{\kappa v^*} + \frac{ln\left[\frac{z_{0\mathrm{m}}}{z_{0\,V,H}}\right]}{\kappa v^*} = \frac{ln\left[\frac{z}{z_{0\mathrm{m}}}\right]^2}{\kappa^2 v_{g,x}(z)} + \frac{ln\left[\frac{z}{z_{0\mathrm{m}}}\right] ln\left[\frac{z_{0\mathrm{m}}}{z_{0\,V,H}}\right]}{\kappa^2 v_{g,x}(z)} \quad [57]$$

640

641 A number of equations that relate $z_{0v,H}$ with z_{0m} and v^* have been proposed (see for instance
642 *Yang et al.* [2008]). *Brutsaert* [1982] developed the following relation between z_{0m} and $z_{0v,H}$:

$$\frac{z_{0\,v,H}}{z_{0\mathrm{m}}} = 7.4exp\left[-2.46\left(\frac{v^* z_{0\mathrm{m}}}{\nu}\right)^{0.25}\right] = 7.4exp\left[-2.46\left(\frac{k v_{g,x}(z) z_{0\mathrm{m}}}{ln\left(\frac{z}{z_{0\mathrm{m}}}\right)\nu}\right)^{0.25}\right] \quad [58]$$

643

644 In Figure 2, the calculated resistances using Eq [49], [50], [57], and [58] for different surface
645 roughness lengths, *d* and two wind velocities, $v_{g,x}$, at 2m height above the soil surface are shown.
646 According to these calculations, the total resistance (r_H) decreases with increasing roughness. This
647 can be attributed to the decreasing transfer resistance in the logarithmic/dynamic sublayer with
648 increasing roughness of the soil surface. However, the difference between transfer resistance for

momentum transfer, r_M, and heat/vapor transfer, $r_{V,H}$ (i.e. $r_{B,}$) increases with increasing roughness. For heat/vapor transfer, the effect of larger turbulent diffusivity in the logarithmic/dynamic layer above a rougher soil surface is counteracted by a longer diffusive pathway through a thicker roughness layer. As a consequence, the decrease of the resistance for heat/vapor transfer with increasing surface roughness is less prevalent than the decrease of momentum transfer resistance (Figure 2).

It should be noted that the transfer resistances described above are based on the assumption of a bluff surface with a no-slip boundary condition. As described before, slip conditions may apply at the surface of a porous medium, which can be accounted for by Beavers-Joseph interface boundary conditions. One way to represent these effects is to define a displacement height, similar to what is used to describe momentum, heat, and vapor transfer between vegetated surfaces and the atmosphere. However, this displacement height should be negative. We are at this moment, not aware of any studies that specify such displacement heights for air flow over rough dry porous media.

Semi-coupled porous medium and free flow using potential evaporation rates and soil surface resistances for drying porous medium.

In the sections above, we described how water flow and heat transport in the porous medium and the free flow are coupled at the interface. However, this coupling is often relaxed by specifying or defining state variables a-priori at the interface. When the vapor pressure at the interface is defined to be the saturated vapor pressure, the water flux from the interface into the free flow is::

$$F_{w,pot} = \frac{\rho_{g,sat}^{w}(z=0) - \rho_{g}^{w}\left(z_{ref}\right)}{r_V} \quad [59]$$

where $F_{w,pot}$ is the so-called potential evaporation, which is calculated without considering the porous medium. It represents the 'demand' for water by the atmosphere and can be used as a flux boundary condition in the porous medium as long as the flow in the porous medium can 'supply'

673 the demand. The saturated vapor concentration at the soil surface depends on the soil surface
674 temperature, which is derived from solving the surface energy balance (Eq. [47]). _ENREF_1
675 An additional soil transfer resistance, r_s [s m^{-1}] was introduced to account for a reduction in
676 evaporation when the soil surface dries out and the vapor pressure becomes smaller than the
677 saturated vapor pressure:

$$F_w = \frac{\rho_{g,sat}^w(z = z_{evap}) - \rho_g^w(z_{ref})}{r_V + r_s(\theta_{l,top})} = \beta(\theta_{l,top})F_{w,pot} \quad [60]$$

678
679 where z_{evap} is the depth where evaporation takes place (i.e. where air is assumed to be saturated
680 with vapor) and $\theta_{l,top}$ is the water content of the 'top soil layer'. However, neither z_{evap} nor the
681 thickness of the top soil layer are explicitly defined or simulated. The soil transfer resistance, r_s, is
682 a function of the water content in the top soil layer whereas r_v depends on the free flow conditions.
683 Water transport in the porous medium and into the atmosphere are hence semi-coupled in this
684 approach. The β factor represents the ratio of the aerodynamic resistance to the sum of the soil and
685 aerodynamic resistance. This approach is often used in large scale simulation models to describe
686 the reduction of evaporation from drying bare soil compared with the potential evaporation from
687 wet soil [*Tang and Riley*, 2013a].
688 *Kondo et al.* [1990], *Mahfouf and Noilhan* [1991], and *Vandegriend and Owe* [1994] used a soil
689 transfer resistance term that increases with decreasing surface soil water content to account for the
690 additional resistance for diffusive vapor transfer when the evaporative surface recedes into the soil
691 profile and *Tang and Riley* [2013a] derived a model for the soil transfer resistance based on the
692 vapor diffusivity and liquid water hydraulic conductivity. Experimentally derived soil transfer
693 resistances were smaller than expected, considering the depth of the evaporation surface and the
694 vapor diffusion coefficient. The smaller resistances were attributed to turbulent eddies that
695 propagate into the porous medium and generate upward and downward movement of air and hence
696 an extra opportunity for mixing with incoming air in the upper soil layer [*Farrell et al.*, 1966;

Ishihara et al., 1992; *Kimball and Lemon*, 1971; *Scotter and Raats*, 1969]. It should be noted that *Assouline et al.* [2013] found that the evaporation flux calculated using Ficks' Law and the depth of the evaporation front (i.e. z_{evap}) underestimated the evaporation rate; however turbulent mixing was not recognized in this case as a potentially relevant process. Additional turbulent mixing leads to an additional dispersive flux of gases in the upper soil layer and has been shown to be of importance for the flux of vapor and trace gases from soil [*Baldocchi and Meyers*, 1991; *Maier et al.*, 2012; *Poulsen and Moldrup*, 2006] and soil covered with mulches [*Fuchs and Hadas*, 2011]. The parameterization of this additional mixing due to turbulence in the top soil is not well known and debated.

A second reason for a decrease in evaporation rate from a drying surface is the spatial variation of the vapor pressure at the soil surface at the microscopic scale. When the lateral distance between evaporating water surfaces in pores at the soil surface becomes too large, the reduction of the evaporating water surface when the soil surface dries out cannot be compensated by an increased lateral diffusion of vapor through the viscous or roughness layer [*Haghighi et al.*, 2013; *Shahraeeni et al.*, 2012; *Suzuki and Maeda*, 1968]. In this case, vapor transfer through the viscous or roughness layer rather than vapor transfer within the porous medium is the limiting factor. If this effect is also accounted for by an additional resistance term, experimental results of *Shahraeeni et al.* [2012] suggest that this resistance term increases with decreasing surface soil water content, that it is larger in soils with larger pores, and that the ratio of this resistance term to the resistance for vapor transport from a saturated soil surface increases with increasing wind velocity. It should be noted that a similar relation with wind speed is observed for the ratio of r_B/r_M (see Figure 2).

Soil transfer resistances have been introduced in soil evaporation models. However, using an additional transfer resistance in a model that explicitly considers diffusive vapor transfer in the soil surface layer (e.g. *Saito et al.* [2006]) leads to a double counting of the transfer resistance

through the soil surface layer and therefore a too strong and rapid decrease in the actual evaporation rate from the soil surface.

Threshold formulation of boundary conditions.

In this approach, water transfer between the porous medium and the free flow is either fully controlled by free flow conditions or by water transport in the porous medium. When the free flow controls the transfer, the potential evaporation is used as a flux boundary condition for water flow in the porous medium. When the porous medium controls the flux, a constant water pressure or water content at the surface of the porous medium is defined and the water flux towards the soil surface is calculated by solving the flow equations in the porous medium for a Dirichlet boundary condition. This approach is used in soil models that solve the Richards equation, e.g. Hydrus 1D [*Simunek et al.*, 2008]. There are no exact guidelines to define the critical pressure head, ψ_{crit}, which is kept constant at the porous medium surface. As a rule of thumb, ψ_{crit} should correspond with a pressure head for which the hydraulic conductivity and capacity of the porous medium ($d\theta/d\psi$) become very small so that a smaller ψ_{crit} would hardly influence simulated water contents and water fluxes towards the soil surface. As will be shown in some simulation examples in the accompanying paper, simulated water fluxes are not so sensitive to the exact choice of this critical pressure head.

Summary and Conclusions:

This work presented an overview of concepts with different complexity that can be used to describe the transfer of water and energy from a porous medium into free flow. We identified how the different approaches are related and which simplifications are used. The most comprehensive description of processes considered multi-dimensional flow of liquid and gas phases and transport

of dry air and water components in the porous medium that was coupled consistently acknowledging mechanical, chemical and thermal equilibrium at the interface to a free flow in the gas phase and transport of vapor and heat above the porous medium. Since the direction of the free flow is generally different from the main direction of the flow and transport processes in the porous medium, this comprehensive approach implies a multi-dimensional description of the flow and transport processes.

However, for homogeneous soil surfaces of a sufficiently large fetch, lateral variations in state variables in the free flow become very small. This leads to a first simplification from a multi- to a one dimensional description of the flow and transport processes in which only the vertical components of flow and transport (in the porous medium) are considered and the vertical components of the gas flow in both the porous medium and the free flow are neglected. This implies that in the porous medium transport in the gas phase happens by diffusion only (i.e. air flow is neglected). This assumption allows to couple the water and heat fluxes in the porous medium and in the free-flow at the porous medium interface using transfer resistances that calculate fluxes from states at the soil/free-flow interface and at a defined height in the free-flow.

A second simplification assumes that vapor transport in the porous medium can be neglected leading to the one component one phase or so-called Richards equation. This simplification decouples water from heat fluxes in the porous medium. At the porous-medium free flow interface, the heat balance equation is solved to determine the water flux at the interface. This balance is solved assuming that the vapor concentration at the soil surface is equal to the saturated vapor concentration so that the heat balance equation is in fact decoupled from the water flow equation in the porous medium. The water fluxes that are derived from this heat balance apply therefore only when the soil surface is sufficiently wet.

The third set of simplifications is related to the description of the interactions or the coupling of the water flow in the porous medium, the interface heat balance, and the evaporation from the interface. In a first approach the transfer between the porous medium and free flow is described

772 by threshold boundary conditions that use prescribed fluxes derived from a surface energy balance
773 until a critical threshold water pressure head is reached at the porous medium surface. This so-
774 called Richards equation with threshold boundary conditions is widely used in soil water balance
775 models. During periods when the pressure head at the surface equals the critical pressure head, the
776 dynamics of the evaporation fluxes are completely defined by the hydraulic properties of the
777 porous medium and the water distribution in the porous medium but are decoupled from the
778 dynamics of the evaporative forcing: radiation, free flow velocity, relative humidity and
779 temperature. A second approach, which is often used in large scale simulation models, combines
780 the diurnal dynamics of the evaporation of a wet surface with a soil surface resistance depending
781 on the soil water content and represents a semi-coupling between the dynamics of the evaporative
782 forcing and the flow process in the porous medium.
783 Finally, there are processes that are not represented or resolved in the comprehensive process
784 description that we presented. These processes are parameterized in the vapor transport description
785 in the porous medium and in the transfer resistances for momentum, heat and vapor transfer
786 between the porous medium and the free flow. . Processes like turbulent diffusion and
787 enhancement of thermal vapor diffusion by thermal non-equilibrium within the porous medium
788 are parameterized in the vapor transport. Non-equilibria (thermal and chemical) can be included
789 in the models by adding additional equations that describe the rate with which an equilibrium is
790 reached, typically first-order rates [*Smits et al.*, 2011]. The rate coefficients are in essence
791 additional empirical parameters that need to be estimated, for example by inverse modeling. Since
792 the surface roughness is not represented in the continuum equations, the effect of roughness on the
793 exchange processes needs to be parameterized in the transfer resistances. Because the small scale
794 mechanisms that control the exchange processes at a rough interface differ for momentum vs heat
795 and vapor exchanges, the parameterizations of the respective transfer resistances differ. However,
796 these parameterizations have been derived mainly for bluff surfaces. Therefore, the effect of

vertical (turbulent pumping) and lateral gas flow in the surface layer of the porous medium, which may be important in highly porous mulches, aggregated soils, and dry soils, is not accounted for. Based on this summary, we conclude that the description of evaporation processes in systems where an important lateral variation in fluxes and states can be expected would require a multidimensional representation of the processes in both the porous medium and the free flow. Although this seems at first sight trivial, it is in fact not generally applied. For instance, several studies that investigated the effect of soil heterogeneity on soil water fluxes use a multidimensional description of the flow process in the porous medium but describe the transfer from the soil surface into the atmosphere using transfer resistances that presume laterally homogeneous state variables in the free flow.

The consideration of the vapor transport in the porous medium and its parameterization due to non-represented processes or its indirect representation in transfer resistances between the porous medium and the free flow is another important difference between the presented model concepts. Under which conditions these differences lead to important differences in simulated evaporation needs to be further investigated.

These conclusions are the starting point of accompanying paper in which we will evaluate the impact of lateral variability and the representation of vapor transport in the porous medium on evaporation simulations.

Acknowledgements:

The authors would like to acknowledge the German Science Foundation, DFG. This work is a contribution of the DFG research unit “Multi-Scale Interfaces in Unsaturated Soil” (MUSIS; FOR 1083) and the DFG International Research Training Group NUPUS and the National Science Foundation (NSF EAR-1447533).

The authors would like to thank the editor and the anonymous reviewers for their insightful comments and suggestions that have contributed to improve this paper.

Tables:

Table 1: Overview of the equations that describe processes in the porous medium, the free flow, and the coupling conditions at the porous medium-free flow interface using different degrees of simplifications.

Porous medium equations			
2 component 2 phase	1 component 1.5 phase (nonisothermal)	1 component 1.5 phase (isothermal)	1 component 1 phase (Richards)
Component (dry air and water) and phase (gas and liquid) equations			
$\sum_{\alpha\in(l,g)} \phi \frac{\partial \rho_\alpha X_\alpha^\kappa S_\alpha}{\partial t} + \nabla \cdot \boldsymbol{F}^\kappa = 0$	$\phi \frac{\partial \rho_g X_g^w S_g}{\partial t} + \phi \frac{\partial \rho_l S_l}{\partial t} + \nabla \cdot \boldsymbol{F}^\kappa = 0$ Equivalent formulation: $\frac{\partial \theta_l}{\partial t} + \frac{\partial \theta_v}{\partial t} = \nabla \cdot \left[\left(\boldsymbol{K}_{l,\psi} + \boldsymbol{K}_{v,\psi} \right) \frac{\sigma(T)}{\sigma\left(T_{ref}\right)} \nabla \psi \vert_{Tref} + \boldsymbol{K}_{l,\psi} \boldsymbol{e_z} \right]$ $+ \nabla \cdot \left(\boldsymbol{K}_{l,T} + \boldsymbol{K}_{v,T} \right) \nabla T$	$\frac{\partial \theta_v}{\partial t} + \frac{\partial \theta_l}{\partial t} =$ $\frac{\partial}{\partial z} \cdot \left[\left(K_{l,\psi} + K_{v,\psi} \right) \frac{\partial \psi}{\partial z} + K_{l,\psi} \right]$	$\frac{\partial \theta_l}{\partial t} = \frac{\partial}{\partial z} \cdot \left[K_{l,\psi} \frac{\partial \psi}{\partial z} + K_{l,\psi} \right]$
$\boldsymbol{F}^\kappa = \sum_{\alpha\in(l,g)} \left(\boldsymbol{q}_\alpha \rho_\alpha X_\alpha^\kappa - D_{\alpha,pm}^\kappa \rho_\alpha \frac{M^\kappa}{\overline{M}_\alpha} \boldsymbol{\nabla} x_\alpha^\kappa \right)$	$\boldsymbol{F}^w \approx \boldsymbol{q}_l \rho_l - \boldsymbol{D}_{g,pm}^w \left(S_g \right) \nabla \rho_g^w$		
$\boldsymbol{q}_\alpha = -\frac{k_{r\alpha}(S_\alpha)}{\mu_\alpha} \boldsymbol{k} \cdot \boldsymbol{\nabla} (p_\alpha - \rho_\alpha \boldsymbol{g} \cdot \boldsymbol{z})$	$\boldsymbol{q}_l = -\frac{k_{rl}(S_l)}{\mu_l} \boldsymbol{k} \nabla (p_l - \rho_l \boldsymbol{g} \cdot \boldsymbol{z})$		
Heat equations			
$\sum_{\alpha\in\{l,g\}} \phi \frac{\partial \rho_\alpha u_\alpha S_\alpha}{\partial t} + (1-\phi) \frac{\partial \rho_s c_s T}{\partial t} + \nabla \cdot \boldsymbol{F}_T = 0$			
$\boldsymbol{F}_T = \sum_{\kappa\in\{a,w\}} \sum_{\alpha\in\{l,g\}} \left(\boldsymbol{q}_\alpha \rho_\alpha X_\alpha^\kappa - D_{\alpha,pm}^\kappa \rho_\alpha \frac{M^\kappa}{\overline{M}_\alpha} \nabla x_\alpha^\kappa \right) h_\alpha^\kappa - \lambda_{T,pm} \nabla T$			

Free flow equations	
Mass balance, Reynolds averaged Navier Stokes, component and energy balance	1-D steady state
$\frac{\partial \rho_g}{\partial t} + \nabla \cdot \left[\rho_g \, \overline{\boldsymbol{v}_g}\right] = 0$	
$\frac{\partial (\rho_g \overline{\boldsymbol{v}_g})}{\partial t} + \nabla \cdot \left[\rho_g \, \overline{\boldsymbol{v}_g} \, \overline{\boldsymbol{v}_g} + \, \overline{p_g}\boldsymbol{I} - \left(\mu_{\boldsymbol{g}}^{\boldsymbol{turb}} + \mu_g\right)\left(\nabla \overline{\boldsymbol{v}_g} + \nabla \overline{\boldsymbol{v}_g}^{\boldsymbol{T}}\right)\right] - \rho_g \boldsymbol{g} = 0$	$\frac{d}{dz}\mu_{\boldsymbol{g}}^{\boldsymbol{turb}} \frac{dv_{g,x}}{dz} = 0$
$\frac{\partial \rho_g \overline{X_g^\kappa}}{\partial t} + \nabla \cdot \left(\rho_g \, \overline{\boldsymbol{v}_g} \overline{X_g^\kappa} - \left(D_g^{turb} + D_g^\kappa\right)\rho_g \frac{M^\kappa}{\overline{M_g}} \nabla \overline{x_g^\kappa}\right) = 0$	$\frac{d}{dz} D_{\boldsymbol{g}}^{\boldsymbol{turb}} \frac{d\rho_g^w}{dz} = 0$
$\frac{\partial \rho_g \, \overline{u_g}}{\partial t} + \nabla \cdot \left(\rho_g \, \overline{\boldsymbol{v}_g} \, \overline{h_g} - \left(\lambda_{T,g}^{turb} + \lambda_{T,g}\right)\nabla \overline{T} - \sum_{\kappa \in \{a,w\}} h_g^\kappa \left(D_g^{turb} + D_g^{\kappa,}\right)\rho_g \frac{M^\kappa}{\overline{M_g}} \nabla \overline{x_g^\kappa}\right) = 0$	$\frac{d}{dz} \lambda_{T,g}^{turb} \frac{dT}{dz} = 0$

Coupling conditions at the porous medium free flow interface			
2 component 2 phase	1-D transfer, aerodynamic resistances	Semi-coupled using soil surface resistance	Semi-coupled using threshold
Mechanical transfer			
$\left[\boldsymbol{n}\cdot\left(\{-\rho_g\,\boldsymbol{v}_g\,\boldsymbol{v}_g\,-\boldsymbol{\tau}_g\,-\boldsymbol{\tau}_g^{turb}+p_g\boldsymbol{I}\}\boldsymbol{n}\right)\right]^{ff}=\left[p_g\right]^{pm}$			
$\left[\left(\boldsymbol{v}_g+\frac{\sqrt{k_i}}{\alpha_{BJ}\mu_g}\left(\boldsymbol{\tau}_g\,+\boldsymbol{\tau}_g^{turb}\right)\boldsymbol{n}\right)\cdot\boldsymbol{t}_i\right]^{ff}=0,\quad i\in\{1,\dots,d-1\}$	$\tau=\rho_g\frac{v_{g,x}(z_{ref})-v_{g,x}(z=0)}{r_M}$ $r_M=\frac{z_{ref}\,\rho_g ln\left(\frac{z_{ref}}{z_{0m}}\right)}{\mu_g^{\boldsymbol{turb}}(z_{ref})}$		
Component transfer			
$\left[x_g^\kappa\right]^{ff}=\left[x_g^\kappa\right]^{pm},\quad\kappa\in\{a,w\}$			
$\left[\left(\rho_g\boldsymbol{v}_g X_g^\kappa-\left(D_g\,+D_g^{turb}\right)\rho_g\frac{M^\kappa}{\overline{M}_g}\nabla x_g^\kappa\right)\cdot\boldsymbol{n}\right]^{ff}=-\left[\left(\rho_g\boldsymbol{q}_g X_g^\kappa-D_{g,pm}^\kappa\rho_g\frac{M^\kappa}{\overline{M}_g}\nabla x_g^\kappa+\rho_l\boldsymbol{q}_l X_l^\kappa-D_{l,pm}^\kappa\rho_l\frac{M^\kappa}{\overline{M}_l}\nabla x_l^\kappa\right)\cdot\boldsymbol{n}\right]^{pm}$	$\frac{\rho_g^w(z=0)-\rho_g^w(z_{ref})}{r_V}=\left[q_l\rho_l-D_{g,eff}^w(S_g)\frac{\partial\rho_g^w}{\partial z}\right]^{pm}$ $r_V\approx r_H=r_M+r_B$	$\frac{\rho_{g,sat}^w(z=z_{evap})-\rho_g^w(z_{ref})}{r_V+r_s(\theta_{l,top})}=[q_l\rho_l]^{pm}$	*If $\psi(z=0)>\psi_{crit}$* $\frac{\rho_{g,sat}^w(z=0)-\rho_g^w(z_{ref})}{r_V}=[q_l\rho_l]^{pm}$ *Else $\psi(z=0)=\psi_{crit}$*
Heat transfer			
$[T]^{ff}=[T]^{pm}$			
$\left[\left(\rho_g h_g\boldsymbol{v}_g-\left(\lambda_{T,g}\,+\lambda_{T,g}^{turb}\right)\nabla T-\sum_{\kappa\in\{a,w\}}h_g^\kappa\left(D_g^\kappa\,+D_g^{turb}\right)\rho_g\frac{M^\kappa}{\overline{M}}\nabla x_g^\kappa\right)\cdot\boldsymbol{n}\right]^{ff}=R_n-\left[\left(\sum_{\kappa\in\{a,w\}}\sum_{\alpha\in\{l,g\}}\left(\boldsymbol{q}_\alpha\rho_\alpha X_\alpha^\kappa-D_{\alpha,pm}^\kappa\rho_\alpha\frac{M^\kappa}{\overline{M}_\alpha}\nabla x_\alpha^\kappa\right)h_\alpha^\kappa-\lambda_{T,pm}\nabla T\right)\cdot\boldsymbol{n}\right]^{pm}$	$c_a\frac{T(z=0)-T(z_{ref})}{r_H}+h_g^w\frac{\rho_g^w(z=0)-\rho_g^w(z_{ref})}{r_V}-R_n=\left[-h_g^w D_{g,eff}^w(S_g)\frac{\partial\rho_g^w}{\partial z}+h_l^w\rho_l q_l-\lambda_{T,pm}\frac{\partial T}{\partial z}\right]^{pm}$	$c_a\frac{T(z=0)-T(z_{ref})}{r_H}+h_g^w\frac{\rho_{g,sat}^w(z=z_{evap})-\rho_g^w(z_{ref})}{r_V+r_s(\theta_{l,top})}-R_n=\left[h_l^w\rho_l q_l-\lambda_{T,pm}\frac{\partial T}{\partial z}\right]^{pm}$	*If $\psi(z=0)>\psi_{crit}$* $c_a\frac{T(z=0)-T(z_{ref})}{r_H}+\left(h_g^w-h_l^w\right)\frac{\rho_{g,sat}^w(z=0)-\rho_g^w(z_{ref})}{r_V}-R_n=\left[-\lambda_{T,pm}\frac{\partial T}{\partial z}\right]^{pm}$ *Else:* $c_a\frac{T(z=0)-T(z_{ref})}{r_H}-R_n=\left[\left(h_l^w-h_g^w\right)\rho_l q_l-\lambda_{T,pm}\frac{\partial T}{\partial z}\right]^{pm}$

831

Figures:

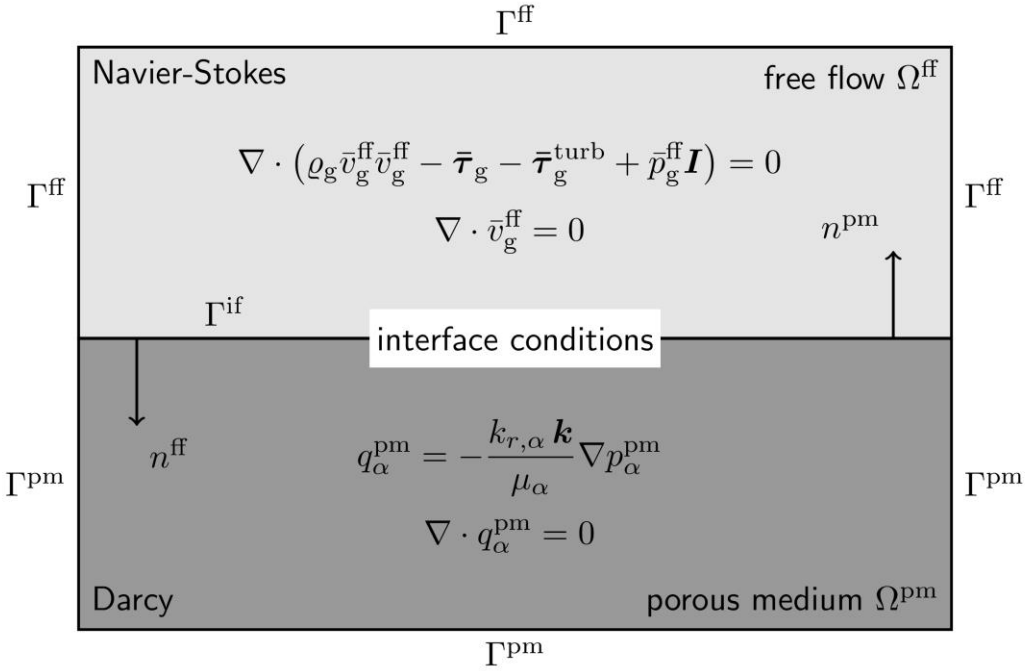

Figure 1: Sketch of the two-domain concept and the notation of the normal vectors (after Mosthaf et al.

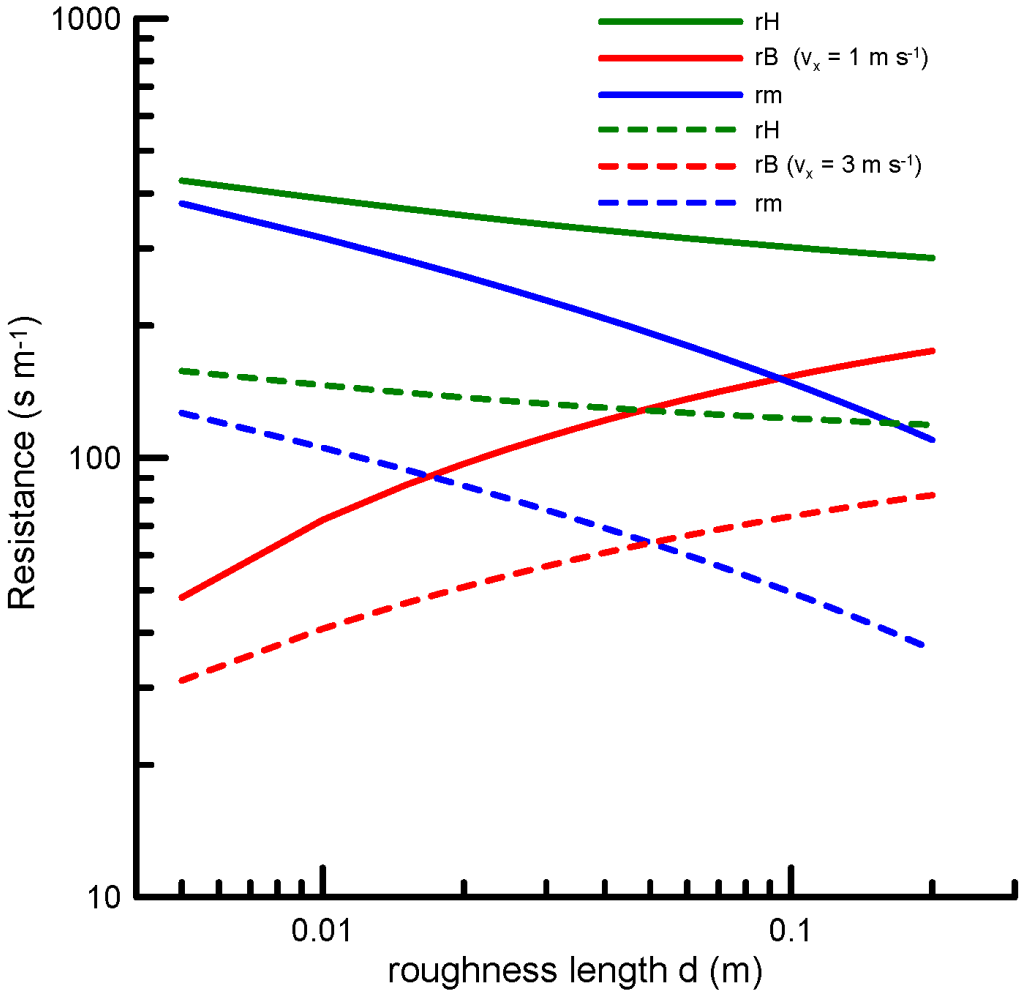

836

837 **Figure 2: Aerodynamic resistances for sensible heat (and vapor) (r_H) and momentum transfer (r_m) through**
838 **the boundary layer as function of the surface roughness length, d, for two different wind speeds, $v_{g,x}$ at 2 m**
839 **height. rB represents the additional resistance for heat transfer compared with momentum transfer.**
840

841

References:

Assouline, S., K. Narkis, and D. Or (2010), Evaporation from partially covered water surfaces, *Water Resour. Res.*, *46*, W10539 doi: 10.1029/2010wr009121.

Assouline, S., S. W. Tyler, J. S. Selker, I. Lunati, C. W. Higgins, and M. B. Parlange (2013), Evaporation from a shallow water table: Diurnal dynamics of water and heat at the surface of drying sand, *Water Resour. Res.*, *49*(7), 4022-4034, doi: 10.1002/wrcr.20293.

Baber, K., K. Mosthaf, B. Flemisch, R. Helmig, S. Müthing, and B. Wohlmuth (2012), Numerical scheme for coupling two-phase compositional porous-media flow and one-phase compositional free flow, *IMA Journal of Applied Mathematics*, *77* (6), 887-909

Bachmann, J., R. Horton, and R. R. van der Ploeg (2001), Isothermal and nonisothermal evaporation from four sandy soils of different water repellency, *Soil Sci. Soc. Am. J.*, *65*(6), 1599-1607.

Bachmann, J., R. Horton, S. A. Grant, and R. R. van der Ploeg (2002), Temperature dependence of water retention curves for wettable and water-repellent soils, *Soil Sci. Soc. Am. J.*, *66*(1), 44-52.

Baldocchi, D. D., and T. P. Meyers (1991), Trace gas-exchange above the floor of a deciduous forest .1. Evaporation and co2 efflux, *J. Geophys. Res.-Atmos.*, *96*(D4), 7271-7285, doi: 10.1029/91jd00269.

Beavers, G. S., and D. D. Joseph (1967), Boundary conditions at a naturally permeable wall, *J. Fluid Mech.*, *30*, 197-&, doi: 10.1017/s0022112067001375.

Bechtold, M., J. Vanderborght, L. Weihermuller, M. Herbst, T. Gunther, O. Ippisch, R. Kasteel, and H. Vereecken (2012), Upward transport in a three-dimensional heterogeneous laboratory soil under evaporation conditions, *Vadose Zone J.*, *11*(2), doi: 10.2136/vzj2011.0066.

Benet, J. C., and P. Jouanna (1982), Phenomenological relation of phase-change of water in a porous-medium - experimental-verification and measurement of the phenomenological coefficient, *Int. J. Heat Mass Transfer*, *25*(11), 1747-1754, doi: 10.1016/0017-9310(82)90154-5.

Bird, R. B., W. E. Stewart, and E. N. Lightfoot (2007), *Transport phenomena*, 905 pp., Wiley, New York.

Boussinesq, J. (1872), Essai sur la théorie des eaux courantes, *Memoires Acad. des Sciences*, *23*(1).

Bristow, K. L., and R. Horton (1996), Modeling the impact of partial surface mulch on soil heat and water flow, *Theor. Appl. Climatol.*, *54*(1-2), 85-98, doi: 10.1007/bf00863561.

Brooks, R. H., and A. T. Corey (1964), Hydraulic properties of porous media.*Rep.*, Fort Collins, Colorado.

Brutsaert, W. (1982), *Evaporation into the atmosphere. Theory, history, and applications*, 299 pp., D.Reidel Publishing Company, Dordrecht.

Brutsaert, W., and S. L. Yu (1968), Mass transfer aspects of pan evaporation, *J. Appl. Meteorol.*, *7*(4), 563-566.

Campbell, G. S. (1985), *Soil physics with basic*, Elsevier, New York.

Campbell, G. S., J. D. Jungbauer, W. R. Bidlake, and R. D. Hungerford (1994), Predicting the effect of temperature on soil thermal-conductivity, *Soil Sci.*, *158*(5), 307-313.

Cass, A., G. S. Campbell, and T. L. Jones (1984), Enhancement of thermal water-vapor diffusion in soil, *Soil Sci. Soc. Am. J.*, *48*(1), 25-32.

Chammari, A., B. Naon, F. Cherblanc, B. Cousin, and J. C. Benet (2008), Interpreting the drying kinetics of a soil using a macroscopic thermodynamic nonequilibrium of water between the liquid and vapor phase, *Dry. Technol.*, *26*(7), 836-843, doi: 10.1080/07373930802135998.

Chung, S. O., and R. Horton (1987), Soil heat and water-flow with a partial surface mulch, *Water Resour. Res.*, *23*(12), 2175-2186, doi: 10.1029/WR023i012p02175.
Cote, J., and J. M. Konrad (2005), A generalized thermal conductivity model for soils and construction materials, *Can. Geotech. J.*, *42*(2), 443-458.
Cote, J., and J. M. Konrad (2009), Assessment of structure effects on the thermal conductivity of two-phase porous geomaterials, *Int. J. Heat Mass Transfer*, *52*(3-4), 796-804, doi: 10.1016/j.ijheatmasstransfer.2008.07.037.
Davis, D. D., R. Horton, J. L. Heitman, and T. S. Ren (2014), An experimental study of coupled heat and water transfer in wettable and artificially hydrophobized soils, *Soil Sci. Soc. Am. J.*, *78*(1), 125-132, doi: 10.2136/sssaj2013.05.0182.
de Vries, D. A. (1958), Simultaneous transfer of heat and moisture in porous media, *Transactions, American Geophysical Union*, *39*(5), 909-916.
de Vries, D. A. (1963), Thermal properties of soils, in *Physics of plant environment*, edited by W. R. V. Wijk, pp. 210-235, North Holland Publ. Co., Amsterdam.
Diamantopoulos, E., and W. Durner (2015), Closed-form model for hydraulic properties based on angular pores with lognormal size distribution, *Vadose Zone J.*, *14*(2), doi: 10.2136/vzj2014.07.0096.
Diaz, F., C. C. Jimenez, and M. Tejedor (2005), Influence of the thickness and grain size of tephra mulch on soil water evaporation, *Agric. Water Manage.*, *74*(1), 47-55, doi: 10.1016/j.agwat.2004.10.011.
Edlefsen, N. E., and A. B. C. Anderson (1943), Thermodynamics of soil moisture, *Hilgardia*, *15*(2), 31-298, doi: 10.3733/hilg.v15n02p031
Farrell, D. A., E. L. Greacen, and C. G. Gurr (1966), Vapor transfer in soil due to air turbulence, *Soil Sci.*, *102*(5), 305-&, doi: 10.1097/00010694-196611000-00005.
Fetzer, T., K. M. Smits, and R. Helmig (2016), Effect of turbulence and roughness on coupled porous-medium/free-flow exchange processes, *Transport Porous Med.*, 1-30, doi: 10.1007/s11242-016-0654-6.
Fuchs, M., and A. Hadas (2011), Mulch resistance to water vapor transport, *Agric. Water Manage.*, *98*(6), 990-998, doi: 10.1016/j.agwat.2011.01.008.
Gurr, C. G., T. J. Marshall, and J. T. Hutton (1952), Movement of water in soil due to a temperature gradient, *Soil Sci.*, *74*, 335-345.
Hadas, A. (1977), Evaluation of theoretically predicted thermal conductivities of soils under field and laboratory conditions, *Soil Sci. Soc. Am. J.*, *41*, 460-466.
Haghighi, E., E. Shahraeeni, P. Lehmann, and D. Or (2013), Evaporation rates across a convective air boundary layer are dominated by diffusion, *Water Resour. Res.*, *49*(3), 1602-1610.
Hahn, S., J. Je, and H. Choi (2002), Direct numerical simulation of turbulent channel flow with permeable walls, *J. Fluid Mech.*, *450* 259-285
Harbeck, G. E. (1962), A practical field technique for measuring reservoir evaporation utilizing mass-transfer theory, *U.S. Geol. Surv. Prof. Paper*, *272E*, 101-105.
Ho, C. K., and S. W. Webb (1998), Review of porous media enhanced vapor-phase diffusion mechanisms, models, and data - does enhanced vapor-phase diffusion exist?, *J. Porous Media*, *1*(1), 71-92.
Hopmans, J. W., J. Simunek, and K. L. Bristow (2002), Indirect estimation of soil thermal properties and water flux using heat pulse probe measurements: Geometry and dispersion effects, *Water Resour. Res.*, *38*(1), doi: 10.1029/2000wr000071.
Horton, R. (1989), Canopy shading effects on soil heat and water-flow, *Soil Sci. Soc. Am. J.*, *53*(3), 669-679.
Ishihara, Y., E. Shimojima, and H. Harada (1992), Water-vapor transfer beneath bare soil where evaporation is influenced by a turbulent surface wind, *J. Hydrol.*, *131*(1-4), 63-104, doi: 10.1016/0022-1694(92)90213-f.

941 Katata, G., H. Nagai, H. Ueda, N. Agam, and P. R. Berliner (2007), Development of a land
942 surface model including evaporation and adsorption processes in the soil for the land-air
943 exchange in arid regions, *J. Hydrometeorol.*, *8*(6), 1307-1324, doi: 10.1175/2007jhm829.1.
944 Kimball, B. A., and E. R. Lemon (1971), Air turbulence effects upon soil gas exchange, *Soil*
945 *Sci. Soc. Am. Proc.*, *35*(1), 16-&.
946 Kondo, J., N. Saigusa, and T. Sato (1990), A parameterization of evaporation from bare soil
947 surfaces, *J. Appl. Meteorol.*, *29*(5), 385-389, doi: 10.1175/1520-
948 0450(1990)029<0385:apoefb>2.0.co;2.
949 Lehmann, P., and D. Or (2009), Evaporation and capillary coupling across vertical textural
950 contrasts in porous media, *Phys. Rev. E*, *80*(4), 046318, doi: 10.1103/PhysRevE.80.046318.
951 Lehmann, P., I. Neuweiler, J. Vanderborght, and H. J. Vogel (2012), Dynamics of fluid
952 interfaces and flow and transport across material interfaces in porous media: Modeling and
953 observations, *Vadose Zone J.*, *11*(3), -, doi: 10.2136/vzj2012.0105.
954 Li, H., F. Wu, H. Zhan, F. Qiu, and W. Wang (2016), The effect of precipitation pulses on
955 evaporation of deeply buried phreatic water in extra-arid areas, *Vadose Zone J.*, *15*, doi:
956 10.2136/vzj2015.09.0127.
957 Lu, S., T. S. Ren, Y. S. Gong, and R. Horton (2007), An improved model for predicting soil
958 thermal conductivity from water content at room temperature, *Soil Sci. Soc. Am. J.*, *71*(1), 8-
959 14, doi: 10.2136/sssaj2006.0041.
960 Lu, S., T. Ren, Y. Gong, and R. Horton (2008), Evaluation of three models that describe soil
961 water retention curves from saturation to oven dryness, *Soil Sci. Soc. Am. J.*, *72*(6), 1542-1546,
962 doi: 10.2136/sssaj2007.0307N.
963 Mahfouf, J. F., and J. Noilhan (1991), Comparative-study of various formulations of
964 evaporation from bare soil using insitu data, *J. Appl. Meteorol.*, *30*(9), 1354-1365, doi:
965 10.1175/1520-0450(1991)030<1354:csovfo>2.0.co;2.
966 Maier, M., H. Schack-Kirchner, M. Aubinet, S. Goffi, B. Longdoz, and F. Parent (2012),
967 Turbulence effect on gas transport in three contrasting forest soils, *Soil Sci. Soc. Am. J.*, *76*(5),
968 1518-1528, doi: 10.2136/sssaj2011.0376.
969 Millington, R., and J. P. Quirk (1961), Permeability of porous solids, *Transactions of the*
970 *Faraday Society*, *57*(8), 1200-1207.
971 Milly, P. C. D. (1982), Moisture and heat-transport in hysteretic, inhomogeneous porous-media
972 - a matric head-based formulation and a numerical-model, *Water Resour. Res.*, *18*(3), 489-498.
973 Milly, P. C. D. (1984), A simulation analysis of thermal effects on evaporation from soil, *Water*
974 *Resour. Res.*, *20*(8), 1087-1098.
975 Modaihsh, A. S., R. Horton, and D. Kirkham (1985), Soil-water evaporation suppression by
976 sand mulches, *Soil Sci.*, *139*(4), 357-361.
977 Monteith, J. L., and M. H. Unsworth (1990), *Principles of environmental physics*, Edward
978 Arnold, London.
979 Moret, D., I. Braud, and J. L. Arrue (2007), Water balance simulation of a dryland soil during
980 fallow under conventional and conservation tillage in semiarid aragon, northeast spain, *Soil*
981 *Tillage Res.*, *92*(1-2), 251-263, doi: 10.1016/j.still.2006.03.012.
982 Mortensen, A. P., J. W. Hopmans, Y. Mori, and J. Simunek (2006), Multi-functional heat pulse
983 probe measurements of coupled vadose zone flow and transport, *Adv. Water Resour.*, *29*(2),
984 250-267, doi: 10.1016/j.advwatres.2005.03.017.
985 Mosthaf, K., R. Helmig, and D. Or (2014), Modeling and analysis of evaporation processes
986 from porous media on the rev scale, *Water Resour. Res.*, *50*(2), 1059-1079, doi:
987 10.1002/2013wr014442.
988 Mosthaf, K., K. Baber, B. Flemisch, R. Helmig, A. Leijnse, I. Rybak, and B. Wohlmuth (2011),
989 A coupling concept for two-phase compositional porous-medium and single-phase
990 compositional free flow, *Water Resour. Res.*, *47*, doi: 10.1029/2011wr010685.

991 Nassar, I. N., and R. Horton (1997), Heat, water, and solute transfer in unsaturated porous media
992 .1. Theory development and transport coefficient evaluation, *Transport Porous Med.*, *27*(1),
993 17-38, doi: 10.1023/a:1006583918576.
994 Nassar, I. N., and R. Horton (1999), Salinity and compaction effects on soil water evaporation
995 and water and solute distributions, *Soil Sci. Soc. Am. J.*, *63*(4), 752-758.
996 Nieber, J. L., and M. F. Walter (1981), Two-dimensional soil-moisture flow in a sloping
997 rectangular region - experimental and numerical-studies, *Water Resour. Res.*, *17*(6), 1722-1730,
998 doi: 10.1029/WR017i006p01722.
999 Nimmo, J. R., and E. E. Miller (1986), The temperature-dependence of isothermal moisture vs
1000 potential characteristics of soils, *Soil Sci. Soc. Am. J.*, *50*(5), 1105-1113.
1001 Noborio, K., K. J. McInnes, and J. L. Heilman (1996), Two-dimensional model for water, heat,
1002 and solute transport in furrow-irrigated soil .2. Field evaluation, *Soil Sci. Soc. Am. J.*, *60*(4),
1003 1010-1021.
1004 Novak, M. D. (2010), Dynamics of the near-surface evaporation zone and corresponding effects
1005 on the surface energy balance of a drying bare soil, *Agric. For. Meteorol.*, *150*(10), 1358-1365,
1006 doi: 10.1016/j.agrformet.2010.06.005.
1007 Nuske, P., V. Joekar-Niasar, and R. Helmig (2014), Non-equilibrium in multiphase
1008 multicomponent flow in porous media: An evaporation example, *Int. J. Heat Mass Transfer*,
1009 *74*, 128-142, doi: 10.1016/j.ijheatmasstransfer.2014.03.011.
1010 Or, D., P. Lehmann, E. Shahraeeni, and N. Shokri (2013), Advances in soil evaporation
1011 physics—a review, *Vadose Zone J.*, *12*(4), doi: 10.2136/vzj2012.0163.
1012 Ouedraogo, F., F. Cherblanc, B. Naon, and J. C. Benet (2013), Water transfer in soil at low
1013 water content. Is the local equilibrium assumption still appropriate?, *J. Hydrol.*, *492*, 117-127,
1014 doi: 10.1016/j.jhydrol.2013.04.004.
1015 Peters, A., and W. Durner (2008), A simple model for describing hydraulic conductivity in
1016 unsaturated porous media accounting for film and capillary flow, *Water Resour. Res.*, *44*(11),
1017 W11417, doi: 10.1029/2008wr007136.
1018 Philip, J. R., and D. A. De Vries (1957), Moisture movement in porous materials under
1019 temperature gradients, *Transactions, American Geophysical Union*, *38*(2), 222-232.
1020 Potter, K. N., R. Horton, and R. M. Cruse (1987), Soil surface-roughness effects on radiation
1021 reflectance and soil heat-flux, *Soil Sci. Soc. Am. J.*, *51*(4), 855-860.
1022 Poulsen, T. G., and P. Moldrup (2006), Evaluating effects of wind-induced pressure
1023 fluctuations on soil-atmosphere gas exchange at a landfill using stochastic modelling, *Waste*
1024 *Manage. Res.*, *24*(5), 473-481, doi: 10.1177/0734242x06066363.
1025 Reshetin, O. L., and S. Y. Orlov (1998), Theory of heat and moisture transfer in a capillary-
1026 porous body, *Tech. Physics*, *43*(2), 263-264, doi: 10.1134/1.1258982.
1027 Rollins, R. L., M. G. Spangler, and D. Kirkham (1954), Movement of soil moisture under a
1028 thermal gradient, *Highway Res. Board Proc.* , *33*, 492-508.
1029 Rose, C. W. (1967), Water transport in soil with a daily temperature wave i. Theory and
1030 experiment, *Aust. J. Soil Res.*, *6*, 31-44.
1031 Ruiz, T., and J. C. Benet (2001), Phase change in a heterogeneous medium: Comparison
1032 between the vaporisation of water and heptane in an unsaturated soil at two temperatures,
1033 *Transport Porous Med.*, *44*(2), 337-353, doi: 10.1023/a:1010773928372.
1034 Saffman, P. G. (1971), Boundary condition at surface of a porous medium, *Stud. Appl. Math.*,
1035 *50*(2), 93-&.
1036 Saito, H., J. Simunek, and B. P. Mohanty (2006), Numerical analysis of coupled water, vapor,
1037 and heat transport in the vadose zone, *Vadose Zone J.*, *5*(2), 784-800, doi:
1038 10.2136/vzj2006.0007.
1039 Sakai, M., S. B. Jones, and M. Tuller (2011), Numerical evaluation of subsurface soil water
1040 evaporation derived from sensible heat balance, *Water Resour. Res.*, *47*, 17, doi: W02547
1041 10.1029/2010wr009866.

Schlüter, S., H.-J. Vogel, O. Ippisch, P. Bastian, K. Roth, H. Schelle, W. Durner, R. Kasteel, and J. Vanderborght (2012), Virtual soils: Assessment of the effects of soil structure on the hydraulic behavior of cultivated soils, *Vadose Zone J.*, *11*(4), -, doi: 10.2136/vzj2011.0174.

Schoups, G., J. W. Hopmans, C. A. Young, J. A. Vrugt, and W. W. Wallender (2005), Multi-criteria optimization of a regional spatially-distributed subsurface water flow model, *J. Hydrol.*, *311*(1-4), 20-48, doi: 10.1016/j.jhydrol.2005.01.001.

Scotter, D. R., and P. A. C. Raats (1969), Dispersion of water vapor in soil due to air turbulence, *Soil Sci.*, *108*(3), 170-&, doi: 10.1097/00010694-196909000-00004.

Seager, R., M. F. Ting, I. Held, Y. Kushnir, J. Lu, G. Vecchi, H. P. Huang, N. Harnik, A. Leetmaa, N. C. Lau, C. H. Li, J. Velez, and N. Naik (2007), Model projections of an imminent transition to a more arid climate in southwestern north america, *Science*, *316*(5828), 1181-1184, doi: 10.1126/science.1139601.

Seneviratne, S. I., D. Lüthi, M. Litschi, and C. Schär (2006), Land-atmosphere coupling and climate change in europe, *Nature*, *443*(7108), 205-209, doi: 10.1038/nature05095

Shahraeeni, E., and D. Or (2011), Thermo-evaporative fluxes from heterogeneous porous surfaces resolved by infrared thermography, *Water Resour. Res.*, *46*, W09511, doi: 10.1029/2009wr008455.

Shahraeeni, E., and D. Or (2012), Pore scale mechanisms for enhanced vapor transport through partially saturated porous media, *Water Resour. Res.*, *48*, doi: 10.1029/2011wr011036.

Shahraeeni, E., P. Lehmann, and D. Or (2012), Coupling of evaporative fluxes from drying porous surfaces with air boundary layer: Characteristics of evaporation from discrete pores, *Water Resour. Res.*, *48*, doi: 10.1029/2012wr011857.

Shepherd, R., and R. J. Wiltshire (1995), An analytical approach to coupled heat and moisture transport in soil, *Transport Porous Med.*, *20*(3), 281-304, doi: 10.1007/bf01073177.

Shokri, N., P. Lehmann, and D. Or (2009), Critical evaluation of enhancement factors for vapor transport through unsaturated porous media, *Water Resour. Res.*, *45*, doi: 10.1029/2009wr007769.

Shuttleworth, W. J. (2012), *Terrestrial hydrometeorology*, Wiley-Blackwell.

Sillon, J. F., G. Richard, and I. Cousin (2003), Tillage and traffic effects on soil hydraulic properties and evaporation, *Geoderma*, *116*(1-2), 29-46, doi: 10.1016/s0016-7061(03)00092-2.

Simunek, J., M. Sejna, H. Saito, M. Sakai, and M. T. van Genuchten (2008), The hydrus-1d software package for simulating the movement of water, heat, and multiple solutes in variably saturated media, version 4.08*Rep.*, 330 pp, Department of Environmental Sciences, University of California Riverside, Riverside.

Smits, K. M., A. Cihan, T. Sakaki, and T. H. Illangasekare (2011), Evaporation from soils under thermal boundary conditions: Experimental and modeling investigation to compare equilibrium- and nonequilibrium-based approaches, *Water Resour. Res.*, *47*, doi: W05540 10.1029/2010wr009533.

Smits, K. M., A. Cihan, T. Sakaki, S. E. Howington, J. F. Peters, and T. H. Illangasekare (2013), Soil moisture and thermal behavior in the vicinity of buried objects affecting remote sensing detection: Experimental and modeling investigation, *IEEE Trans. Geosci. Remote Sensing*, *51*(5), 2675-2688, doi: 10.1109/tgrs.2012.2214485.

Sophocleous, M. (1979), Analysis of water and heat flow in unsaturated - saturated porous media, *Water Resour. Res.*, *15*(5), 1195-1206.

Suzuki, M., and S. Maeda (1968), On the mechanism of drying granular beds: Mass transfer from discontinuous source, *J. Chem. Eng. Jpn.*, *1*(1), 26-31.

Tang, J. Y., and W. J. Riley (2013a), A new top boundary condition for modeling surface diffusive exchange of a generic volatile tracer: Theoretical analysis and application to soil evaporation, *Hydrol. Earth Syst. Sci.*, *17*(2), 873-893, doi: 10.5194/hess-17-873-2013.

Tang, J. Y., and W. J. Riley (2013b), Impacts of a new bare-soil evaporation formulation on site, regional, and global surface energy and water budgets in clm4, *J. Adv. Model. Earth Syst.*, *5*(3), 558-571, doi: 10.1002/jame.20034.
Tarara, J. M., and J. M. Ham (1999), Measuring sensible heat flux in plastic mulch culture with aerodynamic conductance sensors, *Agric. For. Meteorol.*, *95*(1), 1-13, doi: 10.1016/s0168-1923(99)00021-0.
Tarnawski, V. R., W. H. Leong, and K. L. Bristow (2000), Developing a temperature-dependent kersten function for soil thermal conductivity, *Int. J. Energy Res.*, *24*(15), 1335-1350, doi: 10.1002/1099-114x(200012)24:15<1335::aid-er652>3.0.co;2-x.
Taylor, S. A., and L. Cavazza (1954), The movement of soil moisture in response to temperature gradients, *Soil Sci. Soc. Am. Proc.*, *18*, 351-358.
Trautz, A. C., K. M. Smits, and A. Cihan (2015), Continuum-scale investigation of evaporation from bare soil under different boundary and initial conditions: An evaluation of nonequilibrium phase change, *Water Resour. Res.*, *51*(9), 7630-7648, doi: 10.1002/2014wr016504.
Tuller, M., and D. Or (2001), Hydraulic conductivity of variably saturated porous media: Film and corner flow in angular pore space, *Water Resour. Res.*, *37*(5), 1257-1276.
Unger, P. W., and D. K. Cassel (1991), Tillage implement disturbance effects on soil properties related to soil and water conservation - a literature-review, *Soil Tillage Res.*, *19*(4), 363-382.
van Genuchten, M. T. (1980), A closed-form equation for predicting the hydraulic conductivity of unsaturated soils, *Soil Sci. Soc. Am. J.*, *44*(5), 892-898.
Vandegriend, A. A., and M. Owe (1994), Bare soil surface-resistance to evaporation by vapor diffusion under semiarid conditions, *Water Resour. Res.*, *30*(2), 181-188.
Vereecken, H., M. Vanclooster, M. Swerts, and J. Diels (1991), Simulating water and nitrogen behavior in soils cropped with winter-wheat, *Fertil. Res.*, *27*(2-3), 233-243, doi: 10.1007/bf01051130.
Verstraete, M. M., and S. A. Schwartz (1991), Desertification and global change, *Vegetatio*, *91*(1-2), 3-13.
Wang, K. C., and R. E. Dickinson (2012), A review of global terrestrial evapotranspiration: Observation, modeling, climatology, and climatic variability, *Rev. Geophys.*, *50*, 1-54, doi: 10.1029/2011rg000373.
Warren, A. (1996), Desertification., in *The physical geography of africa*, edited by W. M. Adams, A. S. Goudie and A. R. Orme, pp. 342-355, Oxford University Press Oxford, UK.
White, F. M. (1991), *Viscous fluid flow*, 614 pp., McGraw-Hill.
Wieringa, J. (1993), Representative roughness parameters for homogeneous terrain, *Boundary-Layer Meteorol.*, *63*(4), 323-363, doi: 10.1007/bf00705357.
Wilcox, D. C. (2006), *Turbulence modeling for cfd*, DCW Industries, Inc. .
Xie, Z. K., Y. J. Wang, W. L. Jiang, and X. H. Wei (2006), Evaporation and evapotranspiration in a watermelon field mulched with gravel of different sizes in northwest china, *Agric. Water Manage.*, *81*(1-2), 173-184, doi: 10.1016/j.agwat.2005.04.004.
Yamanaka, T., M. Inoue, and I. Kaihotsu (2004), Effects of gravel mulch on water vapor transfer above and below the soil surface, *Agric. Water Manage.*, *67*(2), 145-155, doi: 10.1016/j.agwat.2004.01.002.
Yang, K., T. Koike, H. Ishikawa, J. Kim, X. Li, H. Z. Liu, S. M. Liu, Y. M. Ma, and J. M. Wang (2008), Turbulent flux transfer over bare-soil surfaces: Characteristics and parameterization, *J. Appl. Meteorol. Climatol.*, *47*(1), 276-290, doi: 10.1175/2007jamc1547.1.
Yuan, C., T. Lei, L. Mao, H. Liu, and Y. Wu (2009), Soil surface evaporation processes under mulches of different sized gravel, *Catena*, *78*(2), 117-121, doi: 10.1016/j.catena.2009.03.002.